N-Lab

Ministry of Science and ICT

1. Introduction to KRISS Plasma Research Lab

2. Crystalline silicon nanoparticle (Q-dot) formation by plasma control

Hyo-Chang Lee

LHC@kriss.re.kr



Supported by
- KRISS
- NST & National Laboratory
- Ministry of Science and ICT
- Ministry of Trade, Industry and Energy

Semiconductor Integrated Metrology Team (National Laboratory)

Advanced Instrumentation

Korea Research Institute of Standards and Science

Korea Research Institute of Standards and Science (KRISS)













Korea Research Institute of Standards and Science (KRISS)

NIST: U.S.A.



PTB: Germany



KRISS: KOREA



NMIJ: Japan



NIM: China



R&D Activities

R&D Activities

- Physical Metrology
- Chemical and Medical Metrology
- Industrial Metrology
- Advanced Instrumentation
- Quantum Technology

Introduction to my team (staff member: 10)

Semiconductor Integrated Metrology Center

<Plasma Technology >

<Process/Materials Evaluation Technology >

<Vacuum & Pump Technology >



KRISS Plasma Research Lab (K-PRL)

▶ Member

Staff researcher



JH Kim
Principal Research Scientist



Hyo-Chang Lee
Principal Research Scientist
Distinguished Research Scientist

Post-doc



김영기

최진석

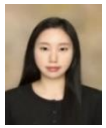
Ph.D course



염희중
박사과정
플라즈마 진단, 전자기시뮬레이션



최은석
석박통합과정
플라즈마 소스 전자기시뮬레이션



윤민영
박사과정
플라즈마 공정 (식각/증착)

김관용
박사과정
플라즈마 진단

MS course



박찬원
석박통합과정
플라즈마 진단내



홍성완
석사과정
플라즈마 소재평가

채광석
석사과정
플라즈마 진단

황도연
석사과정
플라즈마 진단

김성현
석사과정
플라즈마 장비

Alumni

- Dr. DW Kim (KIMM), Dr. BK Na (KFE),
  Dr. M Park (KFE), Dr. prof. KH You (CNU),
  Dr. prof. BH Seo (Embry-Riddle Aeronautical University),
  Dr. DH Choi (Samsung electronics)

▶ about Hyo-Chang Lee

Education & Career

2012. 08 Ph.D., Department of Electrical Engineering, Hanyang University (Korea)
Dissertation: Studies on plasma parameters and electron transport heating in RF biased inductively coupled plasma. Advisor: Prof. Chin-Wook Chung
(Excellence Award for Doctoral Dissertation, *only one selected*)

2012. 09 - 2015. 09 Lecture Professor, Research Professor, Research Fellow
Department of Electrical Engineering, Hanyang University (Korea)

2013. 01 - 2013. 02 Visiting Researcher,
Princeton Plasma Physics Laboratory, Princeton University (USA)

2015. 10 - 2016. 03 Senior Researcher,
Etch Technology Team, Memory division, Samsung Electronics (Korea)

2016. 04 - Now Principal Research Scientist (permanent position)
Korea Research Institute of Standards and Science (Korea)
(Distinguished Research Scientist 2020-2022)

2019. 09 - 2021.08 Adjunct Professor
Department of Electrical Engineering, Hanyang University (Korea)

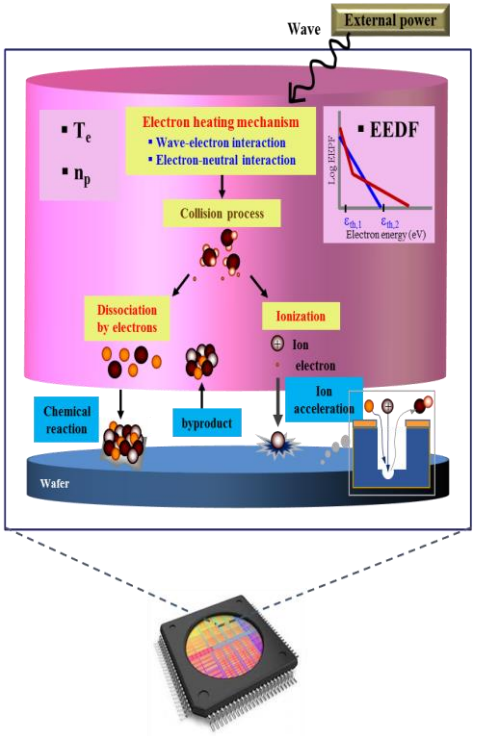
2021. 10 - Now Professional Examiner, Korea Patent Tribunal

❖ Academic/industrial achievement & Activity

- SCI : over 80 papers including Applied Physics Reviews 5, 011108 (2018)
- Patents: more than 30
- IOP Hershkowitz Early Career Award (2020)
- Editorial Board of Plasma Sources Science and Technology (IOP)
- IEEE Senior Member (2018)
- Korean Intellectual Property Office Examination Advisor
- Advisor for the next-generation intelligent semiconductor technology development project
- 2021 Prime Minister Award "Development of Plasma Sensor"(Korea Invention Exhibition)
- Plasma sensor : transfer of technology (one million dollars)

PRL kriss group

* Fundamental study

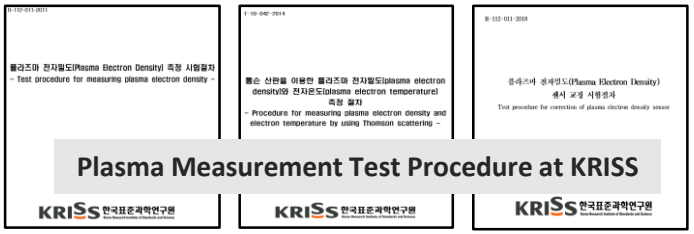


- source
- metrology
- monitoring
- calculation
- processing (etch, depo, ashing, etc)

* Industry support



- **Plasma resistance measurement evaluation (Establishment of KS)** : Measurement of plasma resistance of semiconductor process parts and materials
- **Plasma measurement test report issued**
  : absolute plasma density measurement



- **Establishment of reliability evaluation test bed**
  : Plasma components, equipment reliability evaluation (과기부 N-Lab)
  : Low contamination particle & plasma material reliability evaluation (NRF)
  : Establishment of process sensor reliability evaluation test bed (NST)

Plasma physics & science development,
and semiconductor/display industry technology support

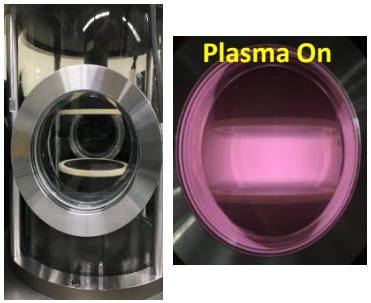
Plasma Group

Plasma equipment

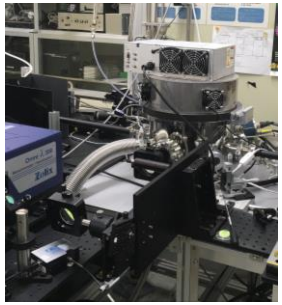
- 300 mm wafer Process (ICP, CCP)



- Symmetric CCP with gap control



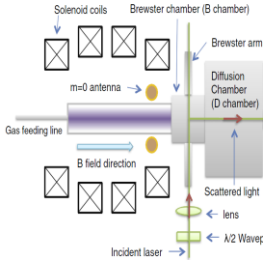
- ICP+CCP



- PECVD (Si)



- Helicon



Plasma Measurement

- Cutoff probe (ne)
- Floating probe (ni, Te)
- Langmuir probe
- Electron energy distribution
- Ion energy distribution
- Laser scattering method (ne, Te)
- OES (plasma light emission)
- PROES (resolution 2 nsec)
- QMS (Radicals)
- PSM (Radical, ion species)

Processing gas

- Ar, Xe, Ne, Kr
- SiH_4, CF_4, C_4F_8, O_2, NF_3, H_2, N_2



Material Analysis

- SEM, Raman, TEM, XPS, PL, Profiler

Cutoff probe & Flat cutoff sensor

Development of plasma diagnostic tool (microwave cut-off probe)

$$n_e = 1.24 \times 10^{10}\left(\frac{f_{cutoff}}{GHz}\right)^2 \ [cm^{-3}]$$

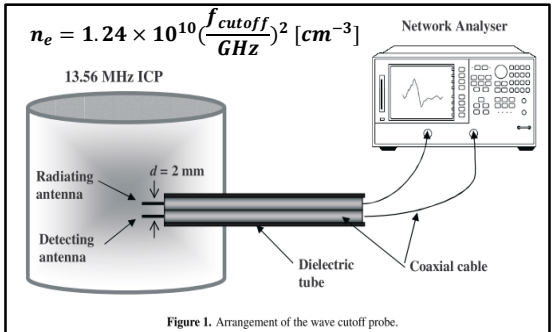
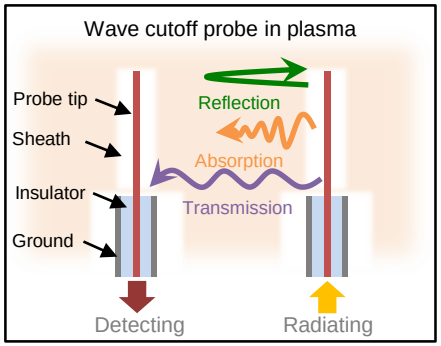


Figure 1. Arrangement of the wave cutoff probe.

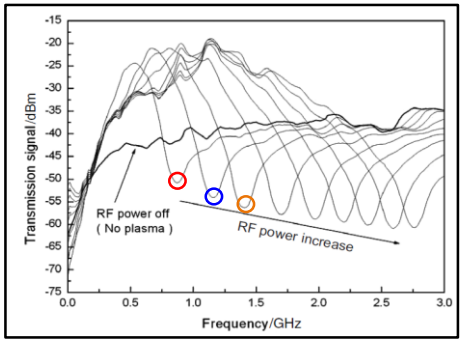


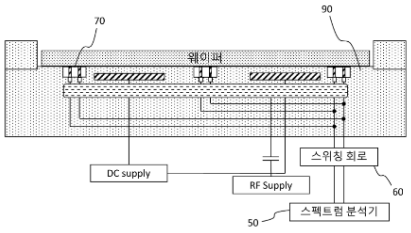
- A *cutoff* occurs in a plasma when the index $\tilde{n} = ck/\omega$ of refraction goes to zero
- A wave is generally reflected at a *cutoff*.
- $\mathbf{B}_0 = 0$ or Ordinary Wave, $\mathbf{E}_1 \parallel \mathbf{B}_0$

$$\omega^2 = \omega_p^2 + c^2k^2$$

- For any finite ω, $\boldsymbol{k} \rightarrow \mathbf{0}$ implies

$$\omega \rightarrow \omega_{cutoff}. \qquad \omega_{pe} = \left(\frac{e^2 n_0}{\varepsilon_0 m}\right)^{\frac{1}{2}}$$



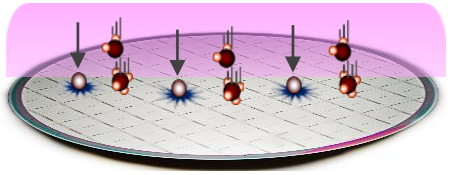


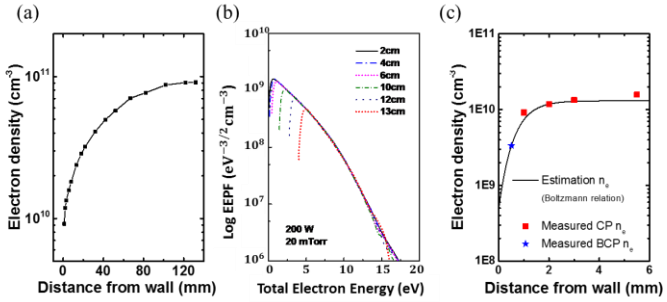


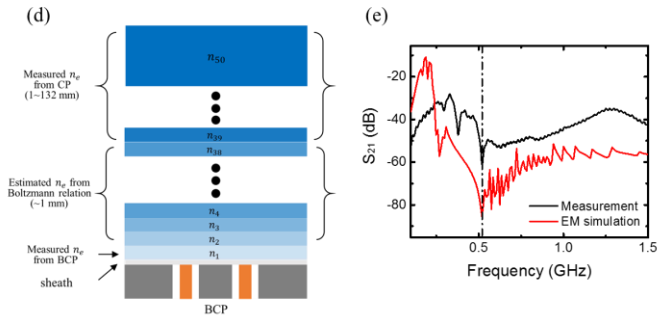
Tens publications from invention to applications

Plasma Sources Sci. Technol. 29 (2020) 035016

- **The amount of plasma incident on the wafer plays a decisive role in the process result**



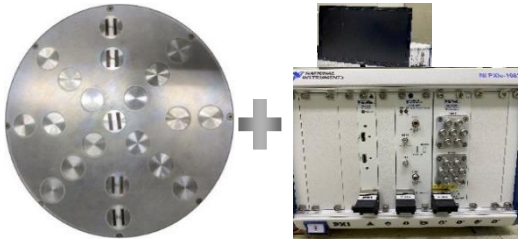




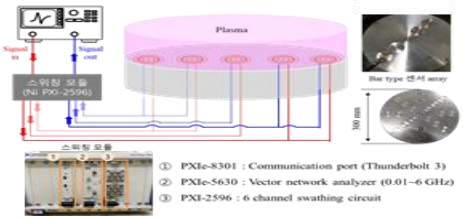
Verify that the BCP diagnostics accurately measure the plasma density of the wafer surface (uncertainty < 2%)

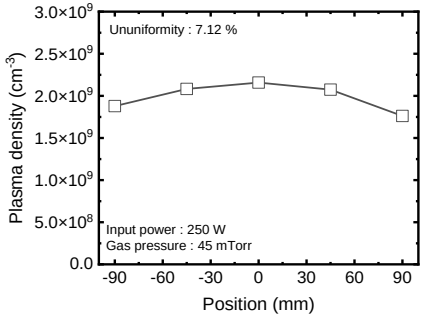
Cutoff probe & Flat cutoff sensor

wafer type & switching | Semiconductor etching process evaluation

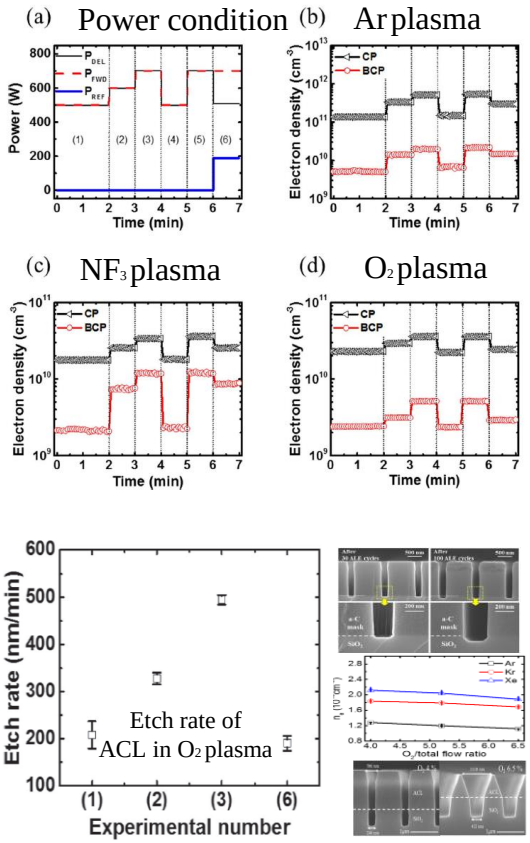


Array sensor Switching module

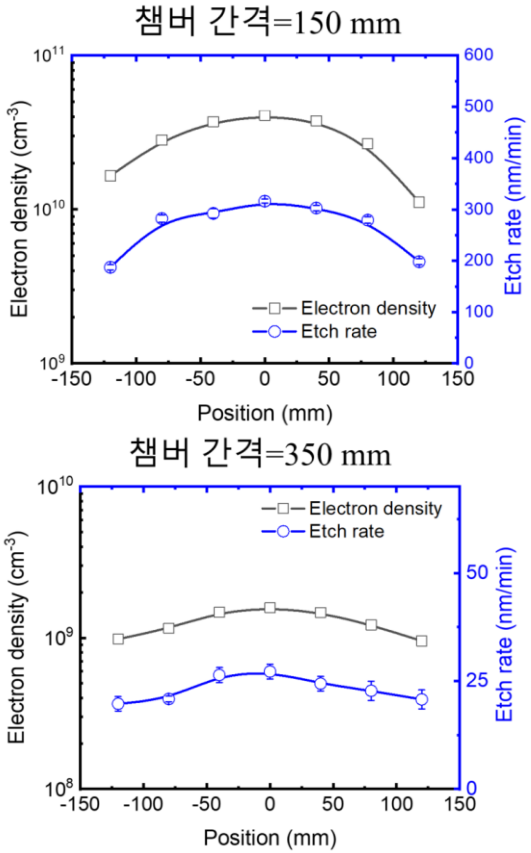




Plasma uniformity measurement

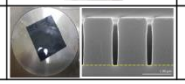


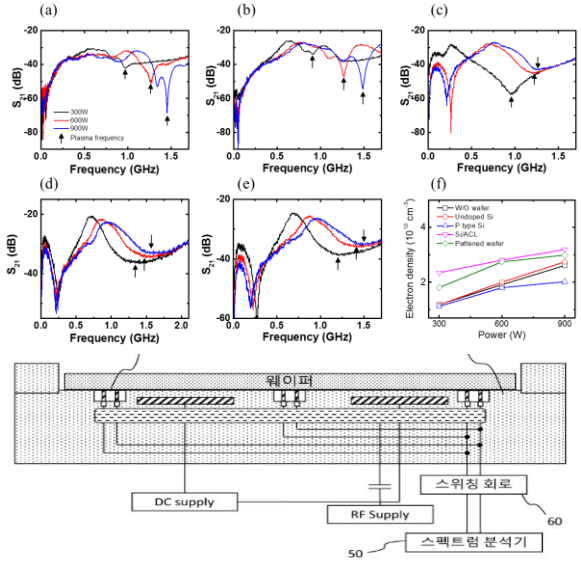
Real-time measurement & ACL etch



Correlation between Plasma Uniformity and Process Results

Cutoff probe & Flat cutoff sensor

Wafer		Resistivity	Thickness
Undoped Si		$> 100\ \Omega \cdot cm$ (ϵ_r =11.7)	$279 \pm 20\ \mu m$
P type Si		$1 \sim 10\ \Omega \cdot cm$ (Boron dopant)	$275 \pm 20\ \mu m$
Amorphous carbon (bulk)		$1.5 \sim 4.5 \times 10^{-3}\ \Omega \cdot cm$ [37, 38]	2 μm (carbon) / wafer (Si)
Patterned wafer		-	1.5 μm (ACL) / 2.5 μm (SiO2) / wafer (Si)



Plasma precision measurement possible even when the wafer is placed on the sensor

: Real-time measurement of plasma density in the wafer area during mass production of semiconductor devices

▪ patent

순번	국내외	출원국가	발명명칭 (국문)	출원일자		등록	
				출원일자	출원번호	등록일자	등록번호
1	국내	KR	평면형 플라즈마 진단 장치	2019-01-31	10-2019-0012572	2020-09-28	10-2162826
2	국내	KR	평면형 플라즈마 진단 장치가 매립된 정전척	2019-03-21	10-2019-0032117	2020-12-15	10-2193694
3	국내	KR	평면형 플라즈마 진단 장치가 매립된 웨이퍼형 플라즈마 진단 장치	2019-03-21	10-2019-0032099	2020-12-15	10-2193678
4	PCT	PCT	평면형 플라즈마 진단 장치, 평면형 플라즈마 진단 장치가 매립된 웨이퍼형 플라즈마 진단 장치, 평면형 플라즈마 진단 장치가 매립된 정전척	2019-04-15	PCT/KR2019/004500		
5	국내	KR	평면형 플라즈마 진단 장치가 매립된 플라즈마 공정 장치	2020-02-20	10-2020-0021312		
6	국외	CN	평면형 플라즈마 진단 장치, 평면형 플라즈마 진단 장치가 매립된 웨이퍼형 플라즈마 진단 장치, 평면형 플라즈마 진단 장치가 매립된 정전척	2020-10-27	2019-80028803		
7	국외	USA	평면형 플라즈마 진단 장치, 평면형 플라즈마 진단 장치가 매립된 웨이퍼형 플라즈마 진단 장치, 평면형 플라즈마 진단 장치가 매립된 정전척	2020-10-23	17/050373		
8	국외	JP	평면형 플라즈마 진단 장치, 평면형 플라즈마 진단 장치가 매립된 웨이퍼형 플라즈마 진단 장치, 평면형 플라즈마 진단 장치가 매립된 정전척	2020-11-17	2021-514264		
9	국외	EU	평면형 플라즈마 진단 장치, 평면형 플라즈마 진단 장치가 매립된 웨이퍼형 플라즈마 진단 장치, 평면형 플라즈마 진단 장치가 매립된 정전척	2020-10-29	2019-912976		
10	국내	KR	플라즈마 이온 밀도 측정 장치와 이를 이용한 플라즈마 진단 장치	2021-02-19	10-2021-0022899		
11	국외	EU	플라즈마 이온 밀도 측정 장치와 이를 이용한 플라즈마 진단 장치	2021-04-07	2021-167098		
12	국외	CN	플라즈마 이온 밀도 측정 장치와 이를 이용한 플라즈마 진단 장치	2021-04-07	2021-10374496		
13	국외	JP	플라즈마 이온 밀도 측정 장치와 이를 이용한 플라즈마 진단 장치	2021-04-01	2021-062613		
14	국외	USA	플라즈마 이온 밀도 측정 장치와 이를 이용한 플라즈마 진단 장치	2021-04-05	17/222937		
15	국내	KR	플라즈마 진단기능을 갖는 정전척	2021-07-06	10-2021-0088782		
16	국내	KR	플라즈마 진단기능 및 유전체 두께 측정기능을 갖는 센서, 이를 구비하는 공정장치 및 공정시스템	2021-07-23	10-2021-0097419		
17	국내	KR	평면형 플라즈마 진단 장치가 매립된 플라즈마 공정 장치				

- FTO
  : 특허 원천성 확인
- Technology valuation

▪ paper

num	Paper title	Journal
1	Flat cutoff probe for real-time electron density measurement in industrial plasma processing	Plasma Sources Sci. Technol. 29 (2020) 035016
2	Circuit model for flat cut-off probes with coplanar capacitance	Plasma Sources Sci. Technol. 30 (2021) 065012

Abstract

The microwave cutoff probe (CP) is an accurate diagnostic technique to measure absolute electron density even in processing gas plasmas. Because this technique needs the installation of two probe tips and a probe body in the plasma chamber, it may cause plasma perturbation in semiconductor plasma processing; this may increase the uncertainty of the measured value. In this work, a flat CP, which is embedded in the substrate chuck or chamber wall, is proposed to measure electron density without plasma perturbation and to monitor processing plasma in real-time. We first evaluated the performance of various types of flat CPs, such as the point CP, ring CP, and bar cutoff probe (BCP), through electromagnetic (EM) field simulation. The BCP showed better performance with clearer cut-off signal characteristics and minimization of noise signals compared with the other probe types. Therefore, we focused on the characteristics of the BCP through experiments and/or EM simulations and concluded the followings: (i) the measured electron densities of the BCP agree well with those of the conventional CP; (ii) the BCP measures the plasma density near the plasma-sheath boundary layer, which is very closely adjacent to the chamber wall or wafer; (iii) it was demonstrated for the first time that the plasma density can be measured, even though the processing wafers such as un-doped silicon, P type silicon, amorphous carbon, or amorphous carbon/SiO_2 patterned wafers were placed on the flat CP; and (iv) we performed real-time measurements of the electron density using the BCP covered with the wafers in plasmas with various process gases, such as Ar, NF_3, and O_2. These results indicate that the chuck-embed-type or wall-type flat CP can be used as a real-time electron density measurement (monitoring) tool during industrial plasma processing, such as during etching, deposition, sputtering or implantation, and the chuck-embed-type flat CP can measure the plasma density impinging on the wafer in real-time without stopping the processing.

▪ 2021 Prime Minister Award for Invention Competition



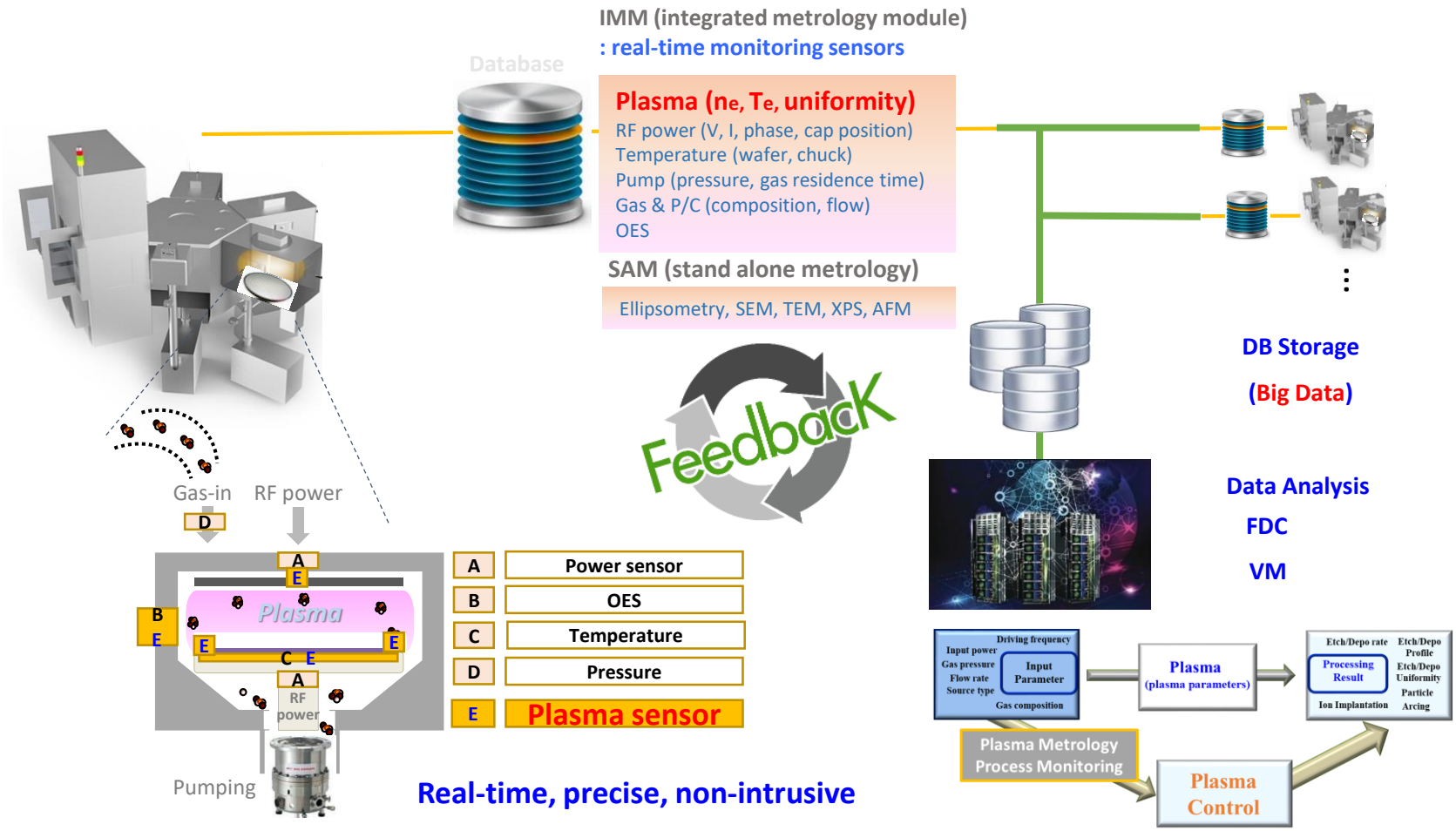


▪ transfer of technology to company (one million dollars)

Sensor-coupled intelligent process equipment

- **Current & Next**

Line width refinement : DRAM < 18 nm, Logic < 7 nm
3D structure: 3D V-NAND/DRAM, Fin/GAA FET



Plasma diagnostics

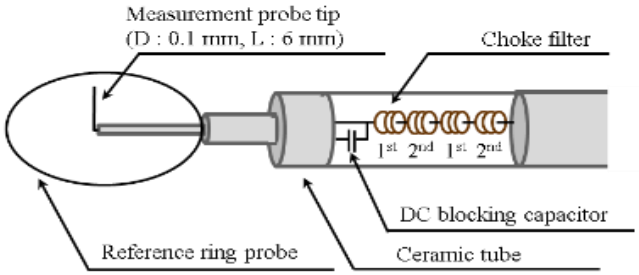
Langmuir probe & EEDF

I-V curve measurement

: compensated single Langmuir probe

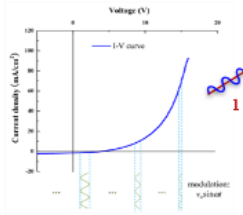
$$n_e = \int_0^{\varepsilon_{max}} f_e(\varepsilon)\, d\varepsilon,$$

$$\langle \varepsilon \rangle = \frac{3}{2} kT_{eff} = \frac{1}{n_e} \int_0^{\varepsilon_{max}} \varepsilon f_e(\varepsilon)\, d\varepsilon$$



EEPF measurement

: AC superposition method

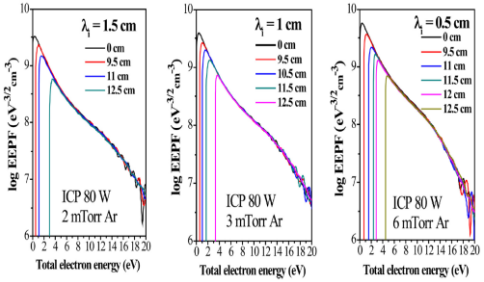


$$I(V + v_0 \sin \omega t) = \left[I(V) + \frac{v_0^2}{4} \frac{d^2 I(V)}{dV^2} + \cdots \right] + \left[v_0 \frac{dI(V)}{dV} + \frac{v_0^3}{8} \frac{d^3 I(V)}{dV^3} + \cdots \right] \sin \omega t + \left[\frac{v_0^2}{4} \frac{d^2 I(V)}{dV^2} + \frac{v_0^4}{48} \frac{d^4 I(V)}{dV^4} + \cdots \right] \sin 2\omega t + \left[\frac{v_0^3}{24} \frac{d^3 I(V)}{dV^3} + \frac{v_0^5}{384} \frac{d^5 I(V)}{dV^5} + \cdots \right] \sin 3\omega t + \cdots$$

$$g_e(\varepsilon) = \frac{8m}{e^2 A} \left(\frac{2\varepsilon}{m} \right)^{1/2} \frac{I_{2\omega}}{v_0^2} \qquad f_e(\varepsilon) = \varepsilon^{1/2} g_e(\varepsilon)$$

$$n_e = \int_0^{\varepsilon_{max}} f_e(\varepsilon)\, d\varepsilon, \quad \langle \varepsilon \rangle = \frac{3}{2} kT_{eff} = \frac{1}{n_e} \int_0^{\varepsilon_{max}} \varepsilon f_e(\varepsilon)\, d\varepsilon$$

Phys. Rev. E 62, 7155 (2000); Phys. Plasmas. 20, 033504 (2013)

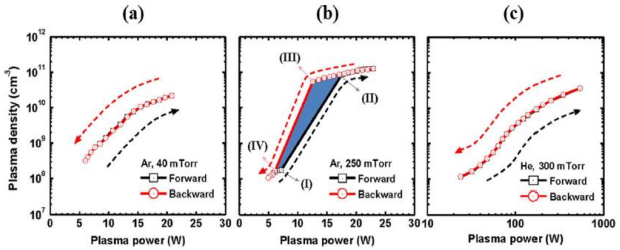


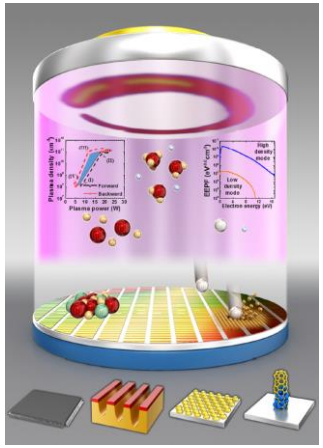
Phys. Plasmas 19, 033514 (2012)

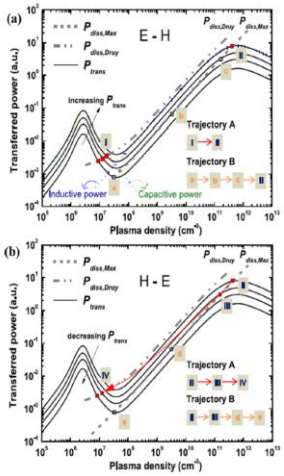
- **Ar, Xe, Ne, Kr**
- **SiH_4, CF_4, C_4F_8, O_2, NF_3, H_2, N_2**
- **Mixture gases**

Study on Unsolved Plasma Physics Based on Plasma Measurements

Hysteresis physics of ICP







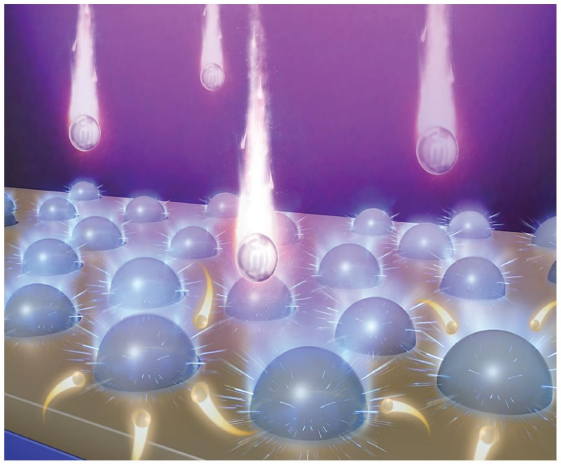
Appl. Phys. Rev. 5, 011108 (2018)

KRISS

Plasma-Surface Interactions

(Structurization mechanism and Control)

Crystalline silicon nanoparticle formation by tailored plasma irradiation : self-structurization, nucleation and growth acceleration, and size control

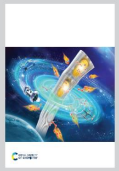


Showcasing research from Dr. Lee`s group at plasma research laboratory, Korea Research Institute of Standards and Science (KRISS), Daejeon, Rep. of Korea.

Crystalline silicon nanoparticle formation by tailored plasma irradiation: self-structurization, nucleation and growth acceleration, and size control

Extremely low energy plasma is utilized to transform the amorphous Si film to crystalline Si nanoparticles. Silicon atoms spontaneously rearrange (self-assembly) to form crystalline nuclei and grow. The energy of the plasma ions bombarding on the material is finely tuned to control the size of the Si nanoparticles in a range of nanometer scale. It is a new and unique phenomenon that the entire film is not crystallized and crystalline nanoparticles (quantum-dots) are generated.

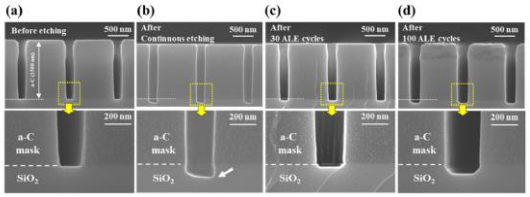
As featured in:



See Hyo-Chang Lee *et al.*, *Nanoscale*, 2021, **13**, 10356.

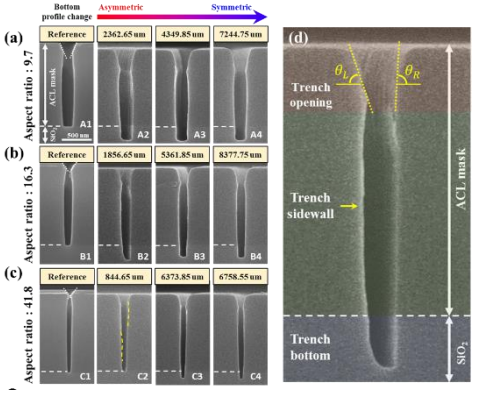
Nanoscale, 13 10356 (2021)

Discharge Physics and Atomic Layer Etching in RF biased ICP



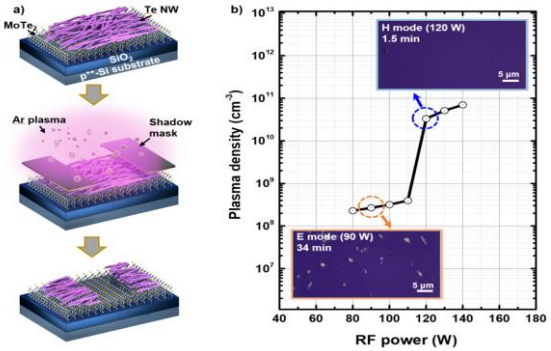
Phys. Plasmas 28, 063504 (2021)

Edge ring effect & High aspect ratio etching mechanism



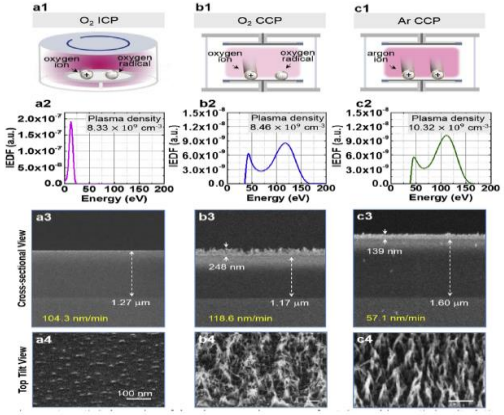
Applied Surface Science (In-press)

Etching of 2D materials



Appl. Surf. Sci. 565, 150521 (2021)

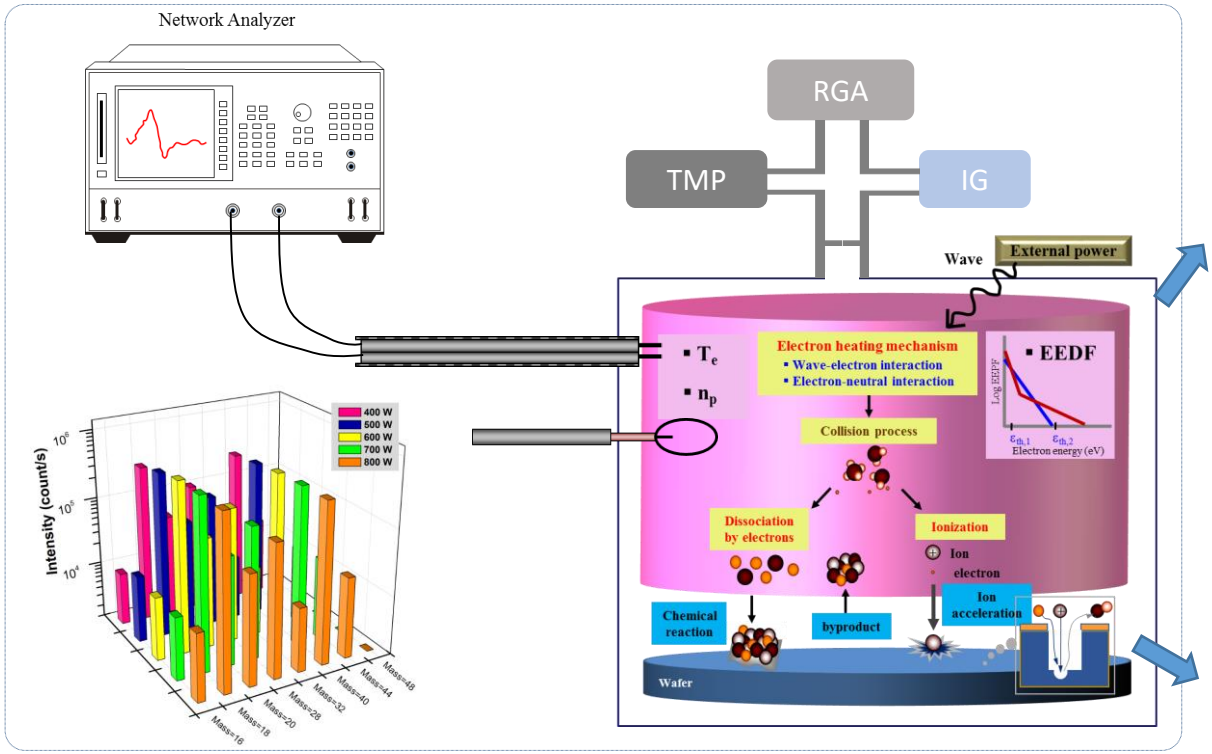
Generation of carbon nanowhiskers, nanotips, and nanodots by controlling plasma environment



Carbon 162 423 (2020)

KRISS

Plasma/Process Measurement Database



- Cutoff probe (ne)
- Floating probe (ion flux)
- QMS (radicals, ions)
- RFA (IEDF)
- LP (EEDF)
- OES
- V-I

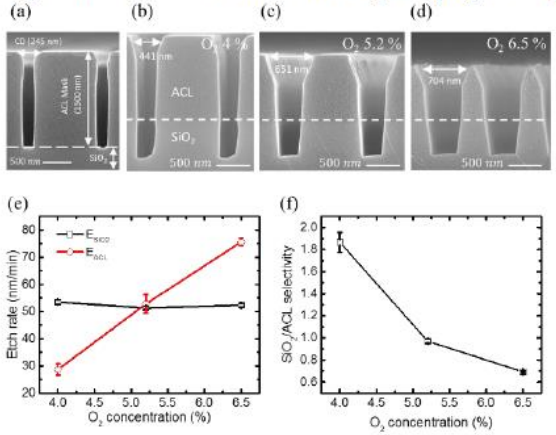
- Processing result
  (etch, deposition, ashing)

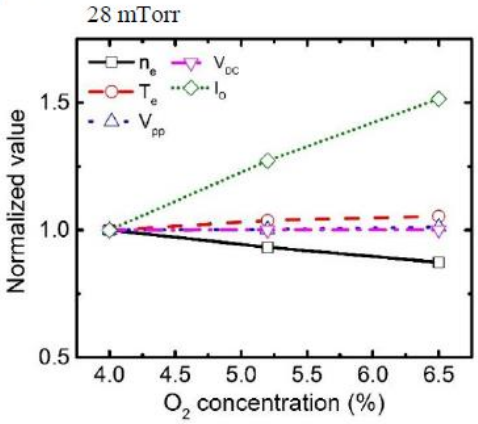
Next-generation process technology development and Development of high-reliability plasma DB

Plasma/Process Measurement Database

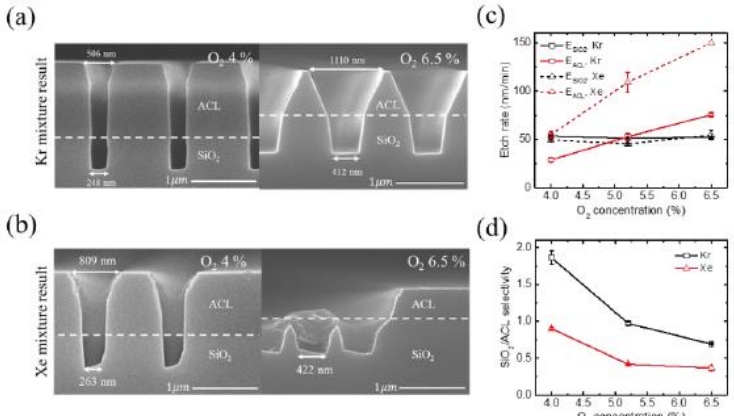
HAR etch & ACL mask damage

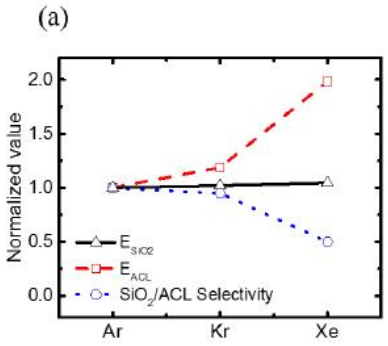
- O_2 미량 효과 in $Ar/O_2/C_4F_8/CH_2F_2$ CCP

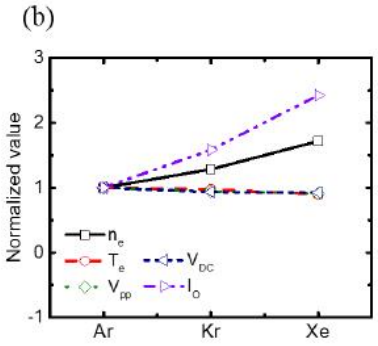




- O_2 미량 효과 in Kr or $Xe/O_2/C_4F_8/CH_2F_2$ CCP





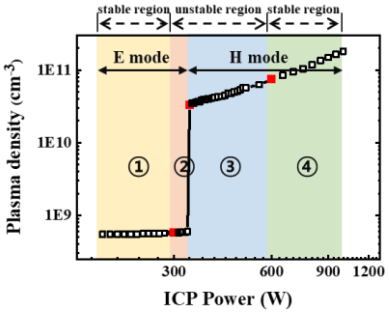


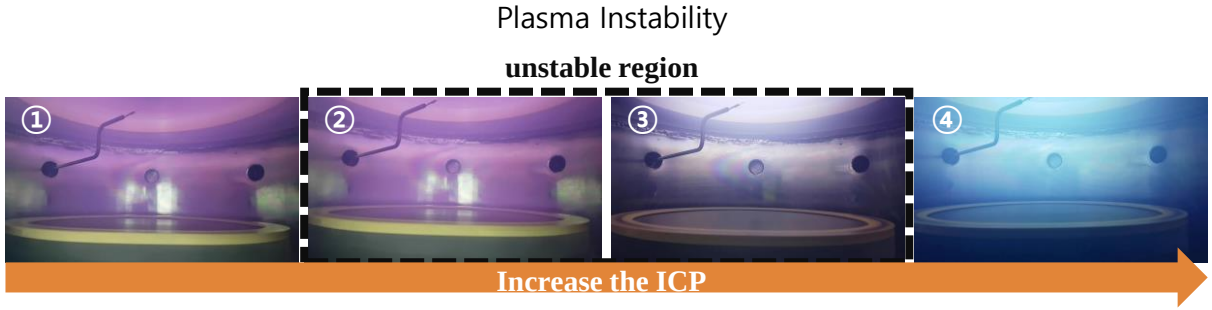
Plasma/Process Measurement Database

Atomic layer etch

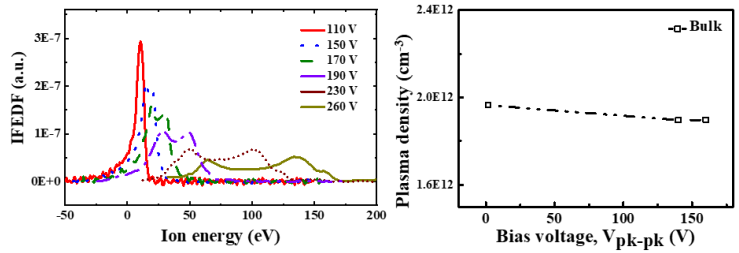
Physics of Plasmas 28, 063504 (2021)
https://aip.scitation.org/doi/10.1063/5.0047811

▶ **Instability in Ar/C_4F_6 mixture plasma**

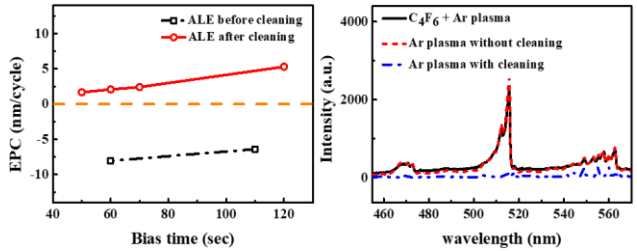




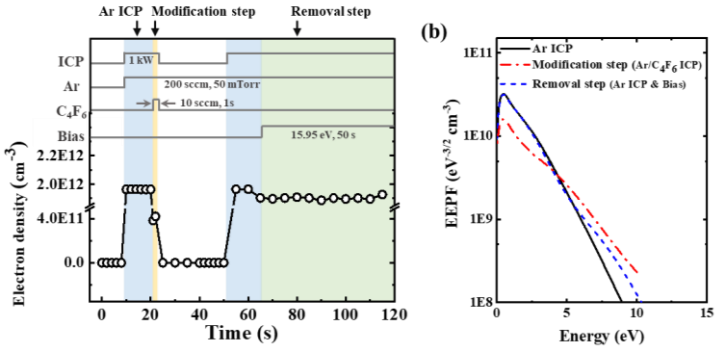
▶ **Ion energy by bias & sputter threshold energy**



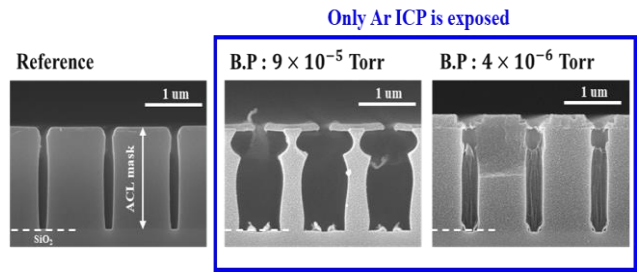
▶ **Chamber wall condition _cleaning**

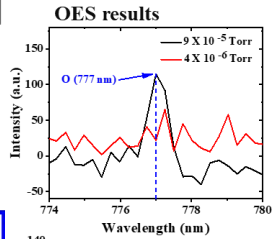


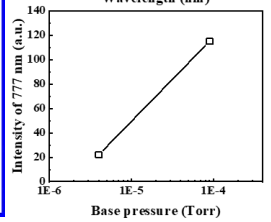
▶ **plasma density & EEDF**



▶ **Base pressure effect**





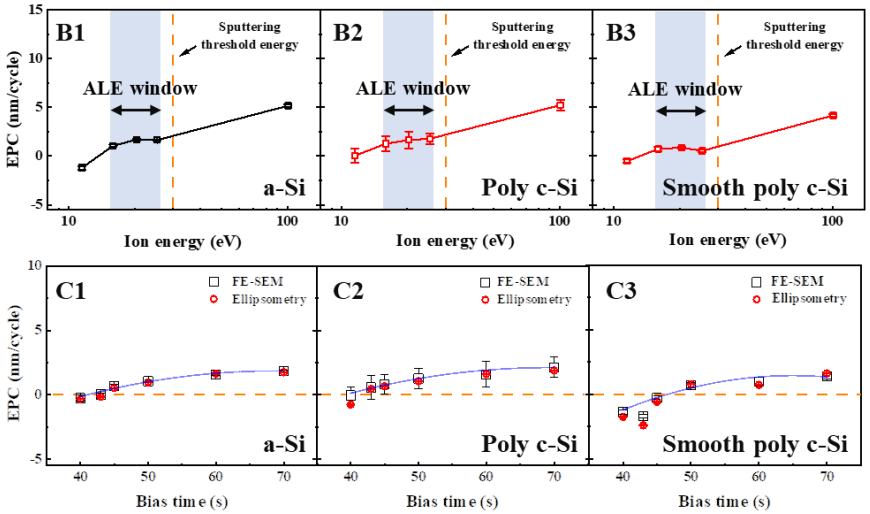


KRISS

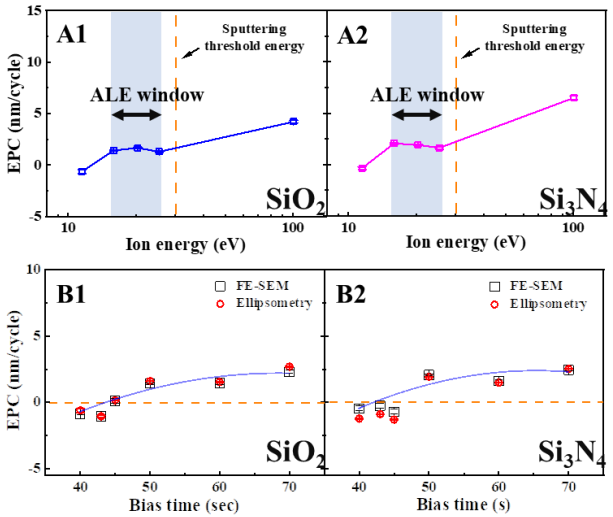
Plasma/Process Measurement Database

Atomic layer etch

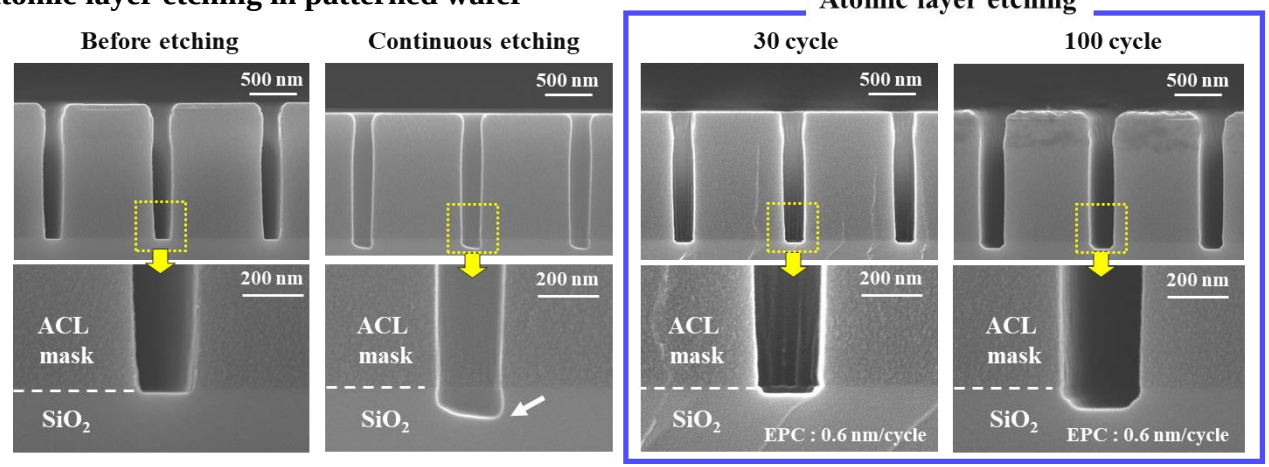
▶ **Quasi- ALE in silicon materials**



▶ **Quasi- ALE in dielectric materials**



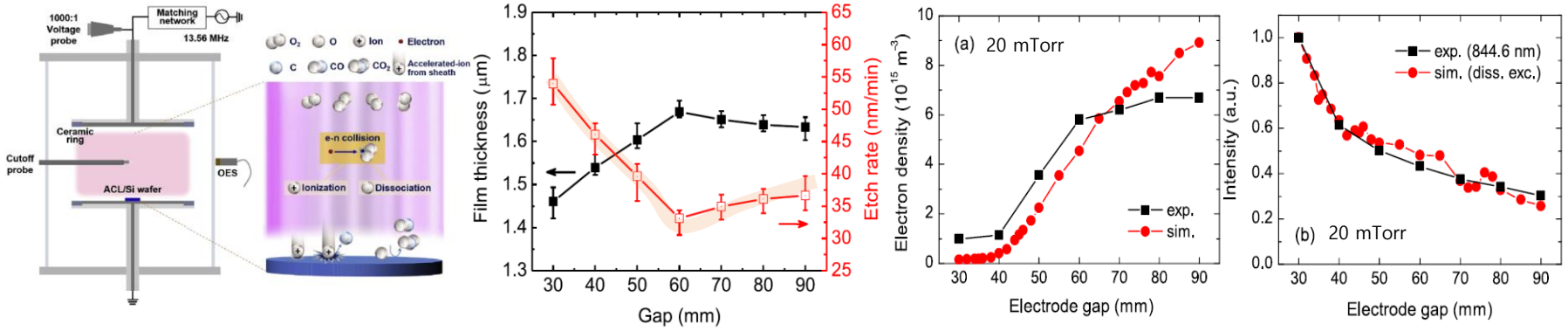
▶ **Atomic layer etching in patterned wafer**



Physics of Plasmas 28, 063504 (2021)
https://aip.scitation.org/doi/10.1063/5.0047811

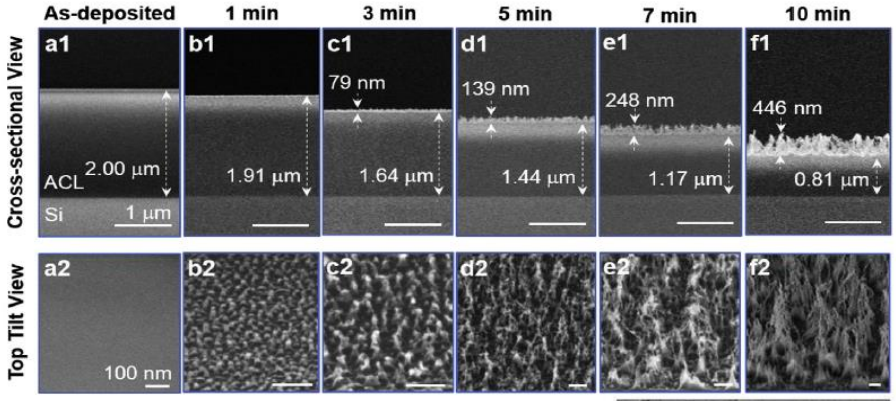
Gap length effect & Surface structurization

- Gap length effect



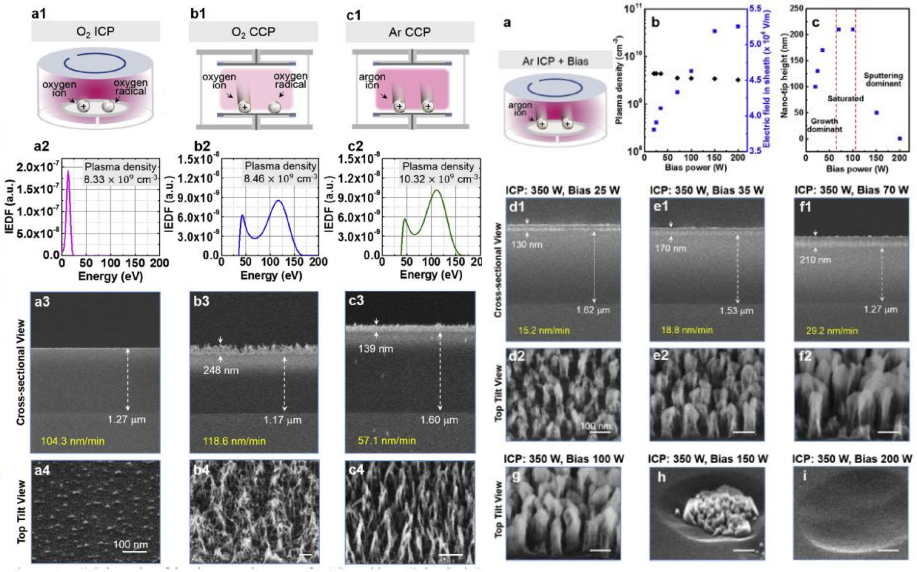
방전 조건에 따른 최적 조건 변동 가능성

- Surface structurization



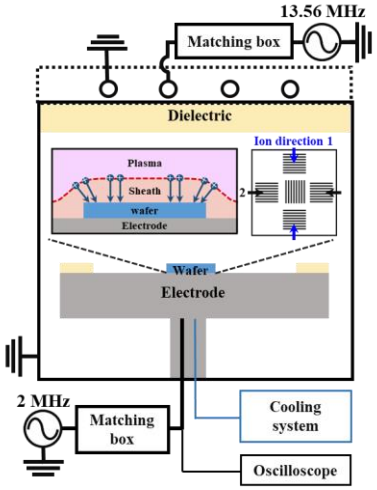
Possibility of micro-arcing

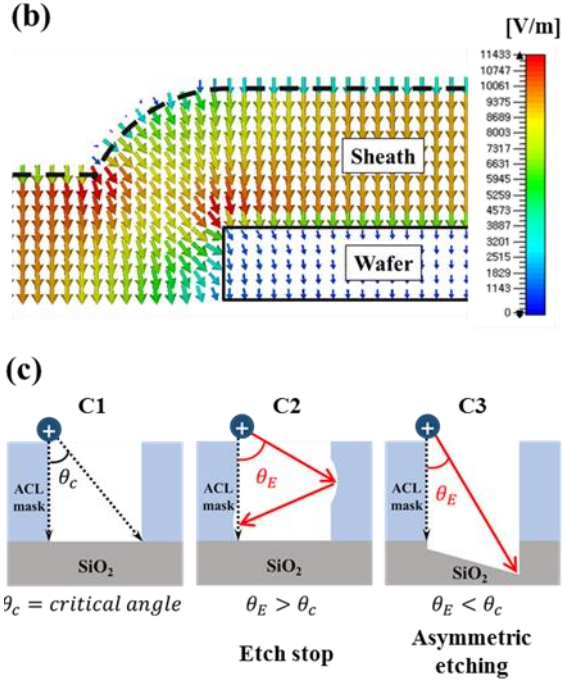
Carbon 162, 423 (2020)

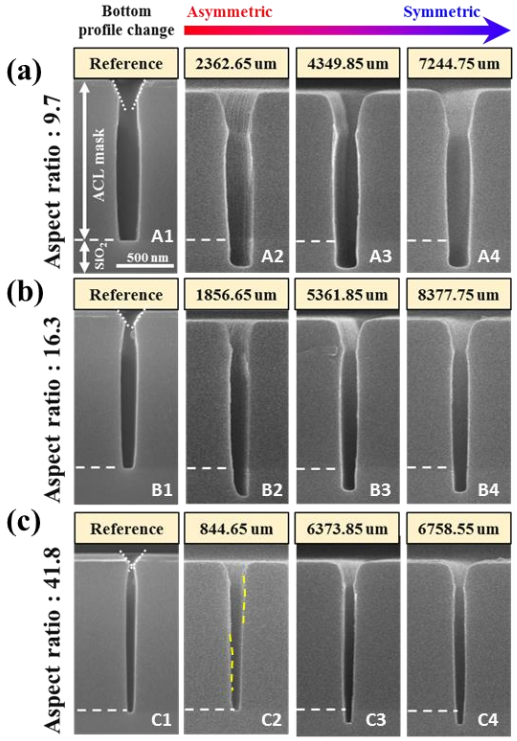


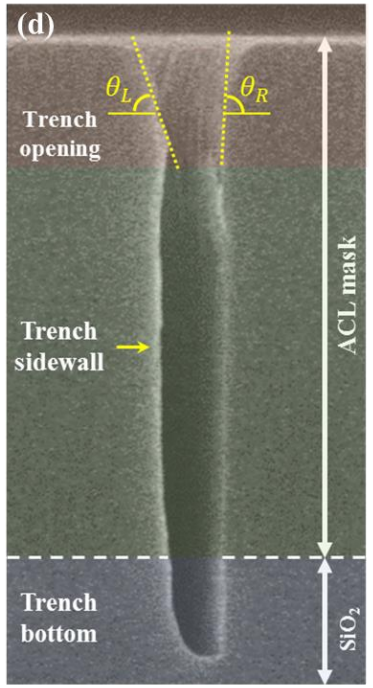
KRISS

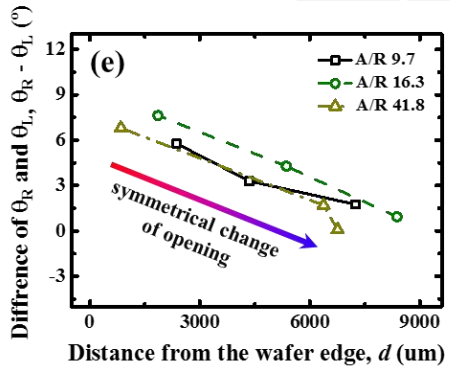
Edge ring effect

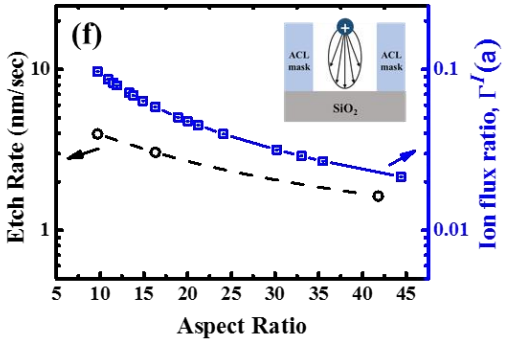






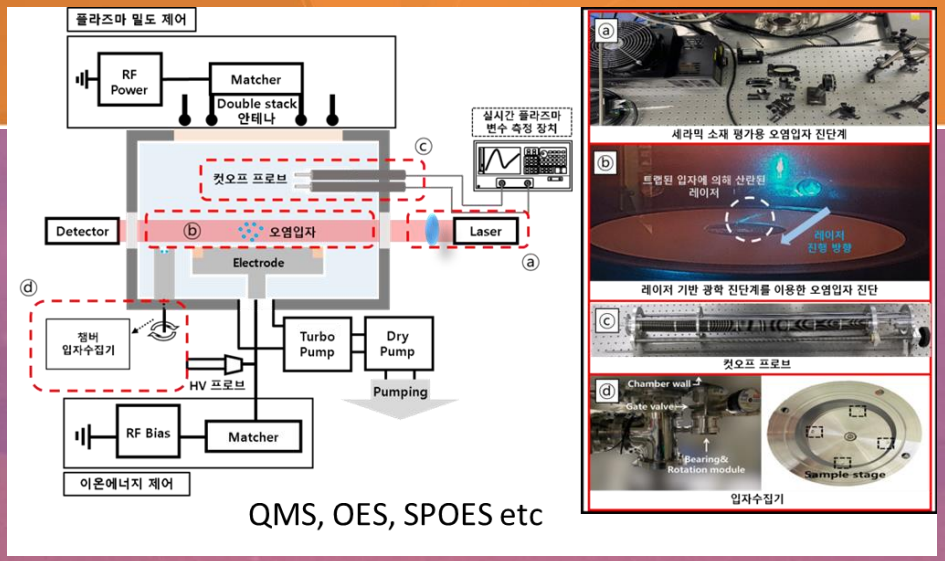






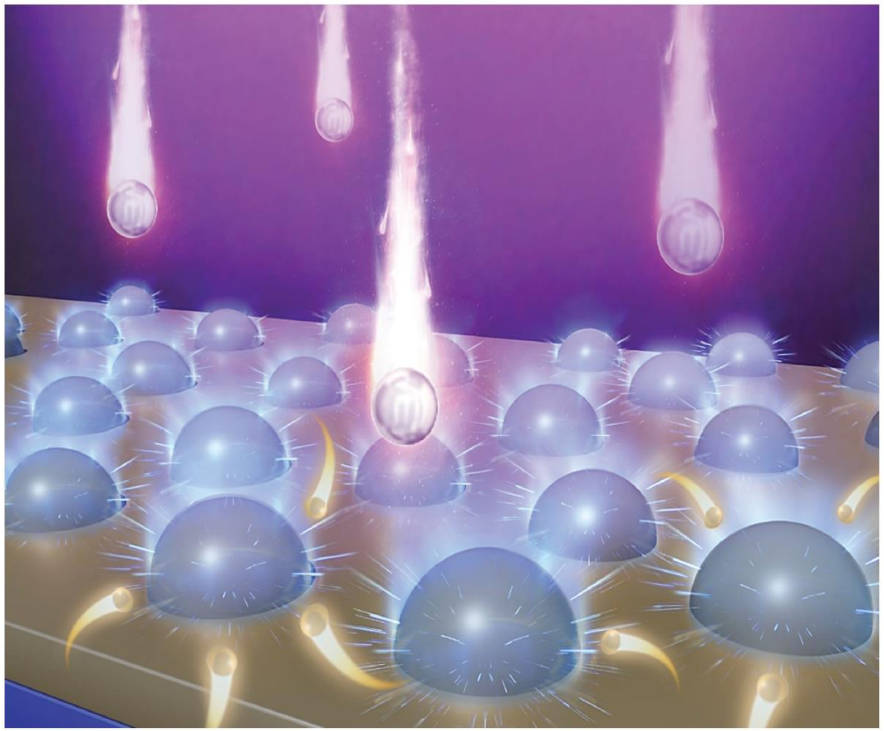
KRISS

Particle control



System for the measurement of plasma resistance of semiconductor process parts and materials

Crystalline silicon nanoparticle (Q-dot) formation by tailored plasma irradiation : self-structurization, nucleation and growth acceleration, and size control



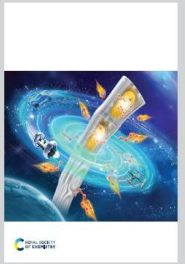
Showcasing research from Dr. Lee`s group at plasma research laboratory, Korea Research Institute of Standards and Science (KRISS), Daejeon, Rep. of Korea.

Crystalline silicon nanoparticle formation by tailored plasma irradiation: self-structurization, nucleation and growth acceleration, and size control

Extremely low energy plasma is utilized to transform the amorphous Si film to crystalline Si nanoparticles. Silicon atoms spontaneously rearrange (self-assembly) to form crystalline nuclei and grow. The energy of the plasma ions bombarding on the material is finely tuned to control the size of the Si nanoparticles in a range of nanometer scale. It is a new and unique phenomenon that the entire film is not crystallized and crystalline nanoparticles (quantum-dots) are generated.

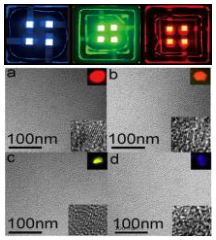
Nanoscale, 13 10356 (2021)

As featured in:

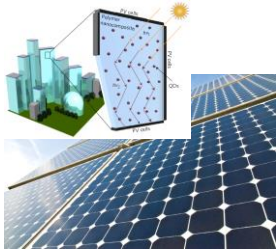


See Hyo-Chang Lee *et al.*, *Nanoscale*, 2021, **13**, 10356.

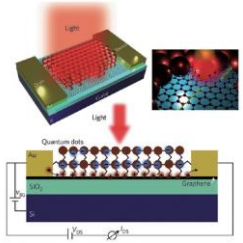
Si NPs Applications



By Zhenhui Kang et al., Adv. Mater., 21, 661–664 (2009)



F. Meinardi et al., Nat. Photonics, 11, 177 (2017)



H. Fang et al., Adv. Sci., 17, 1700323 (2017)

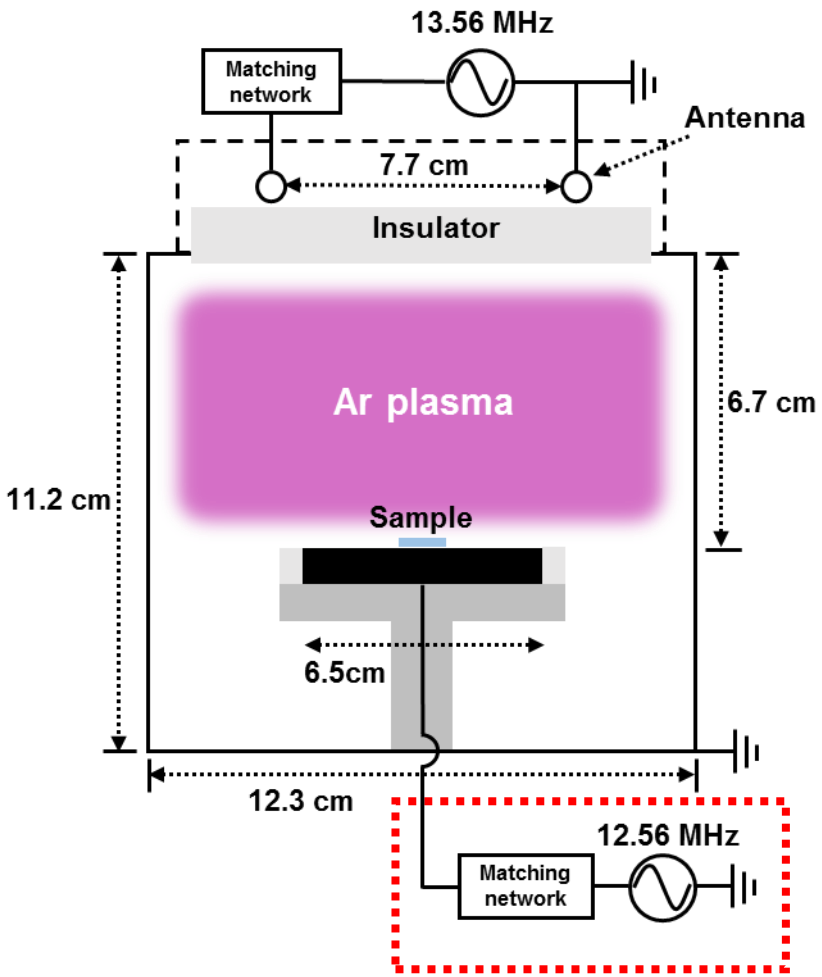
Despite the indirect bandgap of Si, Si nanoparticles (NPs) of 2–6 nm show direct-bandgap (size-dependent) properties in the visible range owing to the quantum confinement effect.[1–9] Thus, Si NPs, as an Earth-abundant and mass-production material, have been utilized in various fields such as photovoltaic devices,[1–4] quantum-dot light-emitting diodes,[5–7] and photodetectors.[10]

For photonic device applications, the synthesis of Si NPs with superior size (2–6 nm) control and high quantum yield is highly important. In terms of quantum yield efficiency, Li et al.[11,12] and Pringle et al.[13] have recently reported the synthesis of Si NPs with ultrahigh photoluminescence (PL) quantum yields over 70,[13] 75,[11] and 90%.[12] So et al.[14] have recently analyzed the emission mechanism of Si NPs with such a high quantum yield in detail. Nevertheless, it is still difficult to control the nanoparticle size finely in the 2–6 nm range.

To date, three types of approach for the fabrication of Si NPs have been developed:
(i) top-down approaches: electrochemical etching of bulk Si,[15,16] breakdown of Si-rich oxides containing Si nanocrystals,[17] and ripple formation by locally applied ion beams on pristine crystalline Si films (above 500 eV)[18,19]
(ii) bottom-up approaches: solution-based precursor reduction[20] and Zintl salt-based approaches;[9,21]
(iii) precursor decomposition and re-assembly approaches: preparation in supercritical fluids,[22] laser pyrolysis,[23] and gas-phase discharge synthesis.[24]

These existing methods require high temperature,[9,17–19,23] use of HF solution,[15,17,23] and an additional process for the uniform redistribution of NPs on the substrate,[9,15–17,20–24] which is necessary for the uniform optical performance in optical applications such as solar cells, quantum-dot LEDs, and plasmonics,[25] and there are difficulties in controlling the size;[18,19] therefore, a new advanced technique to fabricate Si NPs with excellent size control and scalability in nonharsh (low-temperature) and nontoxic environments is highly required.

ICP chamber scheme and experimental condition



➢ Fixed parameters

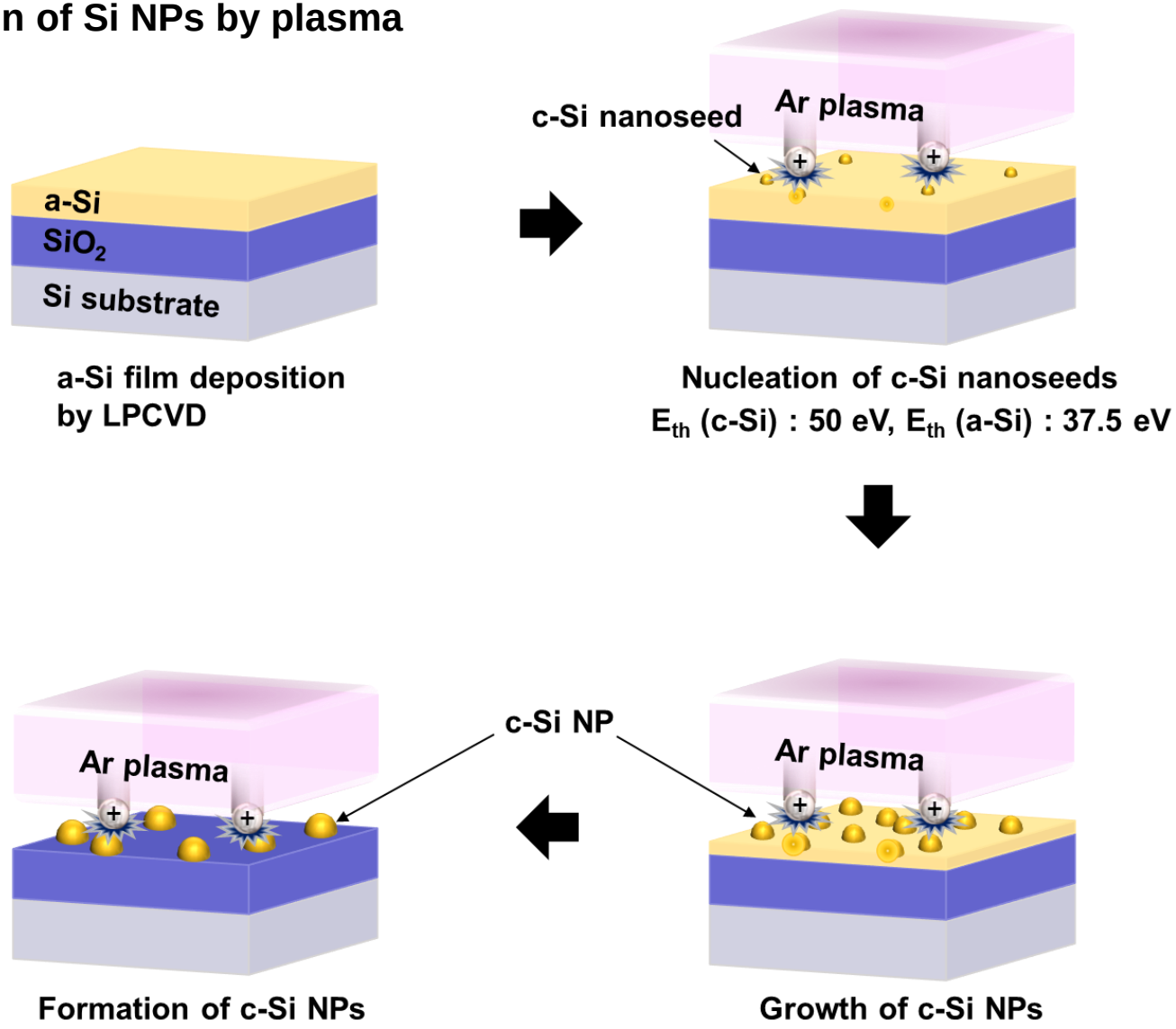
- ICP power: 300 W
- Ar flow rate: 10 sccm
- Working pressure: 20 mTorr
- a-Si (LPCVD) thickness: 13 nm

➢ Variable parameters

- RF bias power of substrate electrode: 5 ~ 11 W
- Plasma exposure time

Formation mechanism

➢ **Generation of Si NPs by plasma**



Formation process of Si NPs by plasma ion bombardment

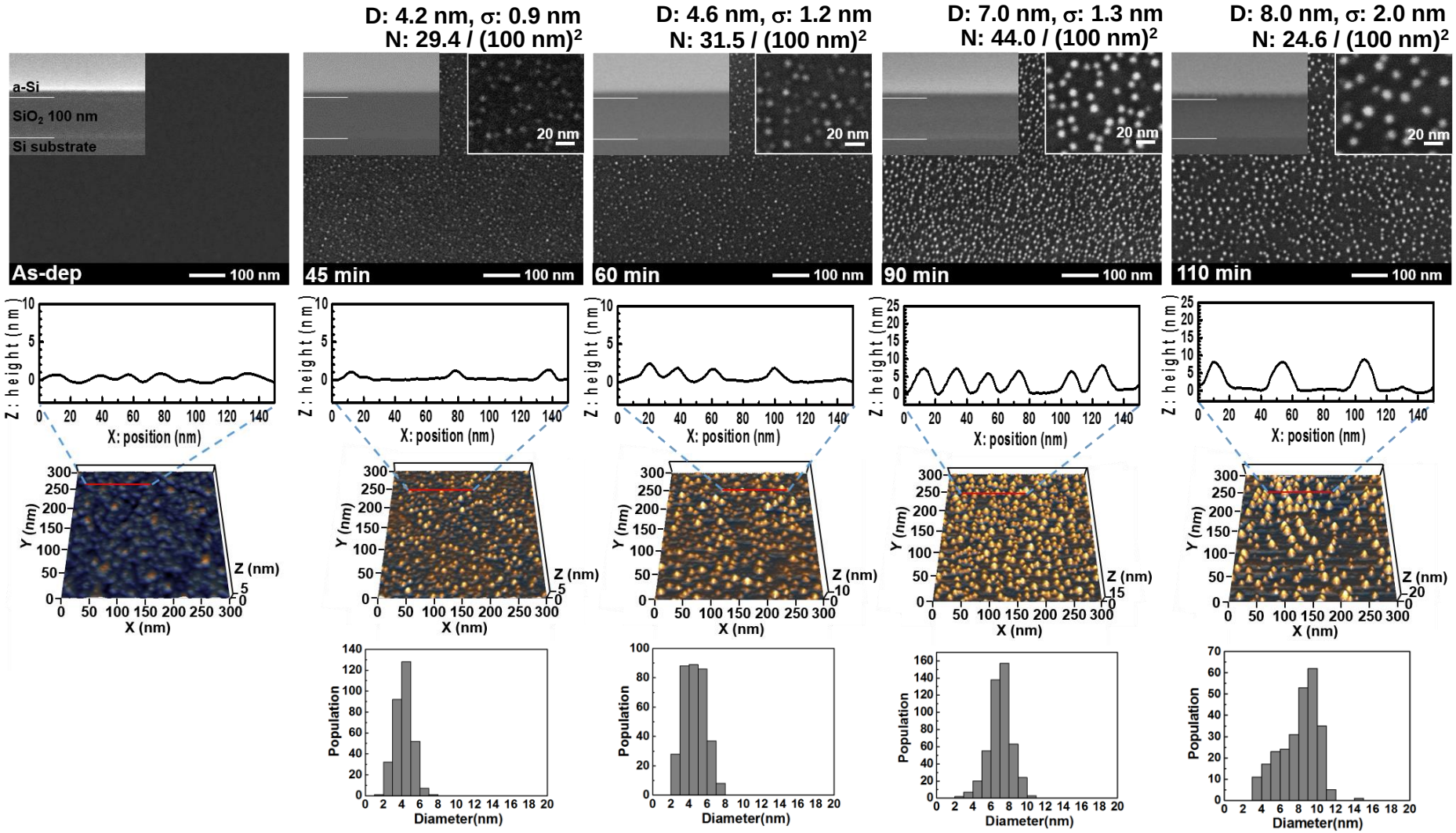


Fig) a-Si films after plasma treatment with bias power of 6 W by times

- With increase in plasma treatment time, nanoseeds grew into larger size of Si NPs.

KRISS

SEM and TEM measurement of Si NP fabricated by plasma

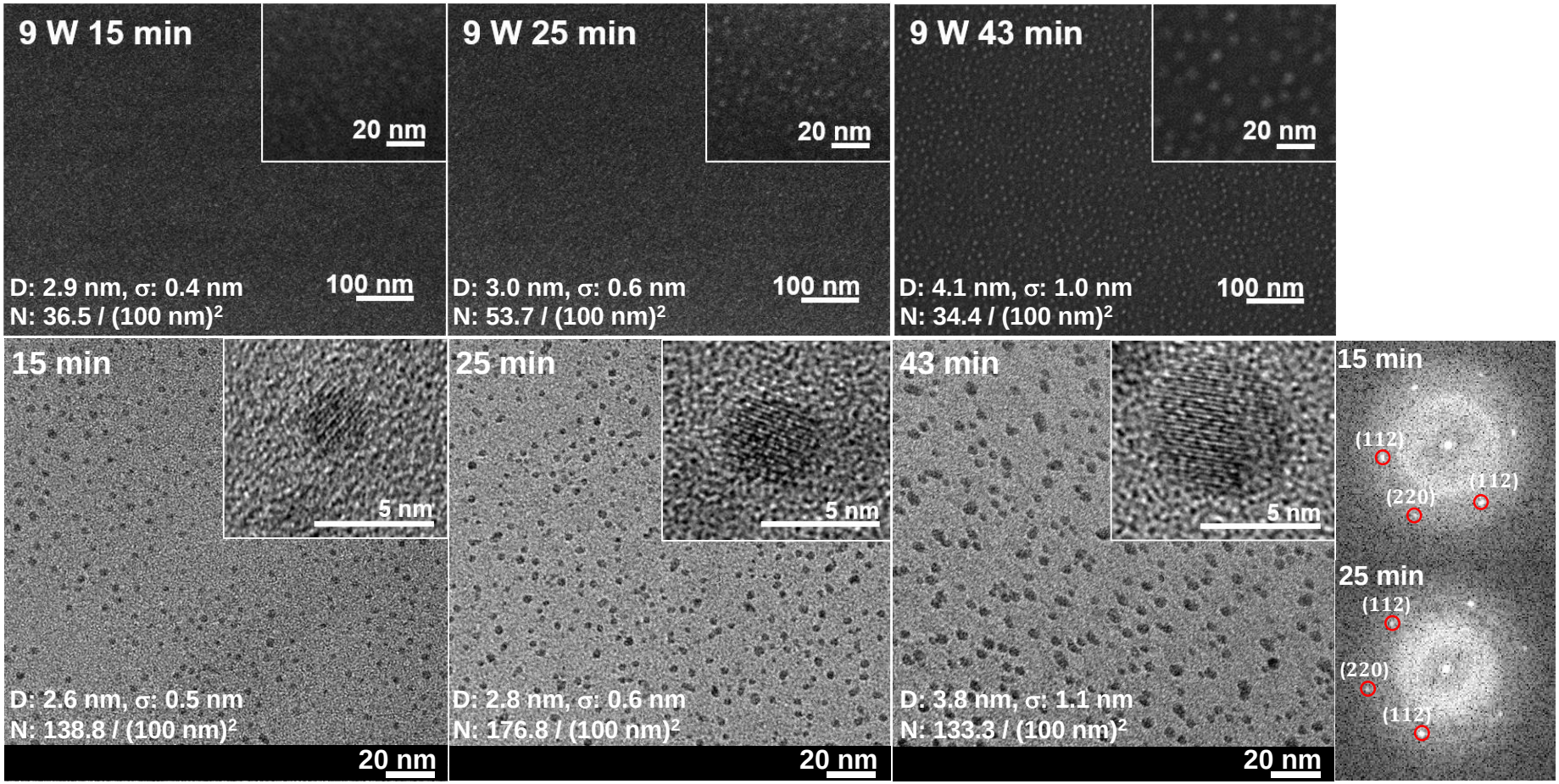


Fig) Plan view SEM images and plan view TEM images and FFT pattern of Si NPs on SiO_2/Si substrate fabricated at RF bias power of 9 W depending on plasma exposure time

- **HRTEM images indicates that NP is crystalline and has a lattice plane spacing of diamond cubic Si.**

Number density and size of Si NP fabricated by plasma

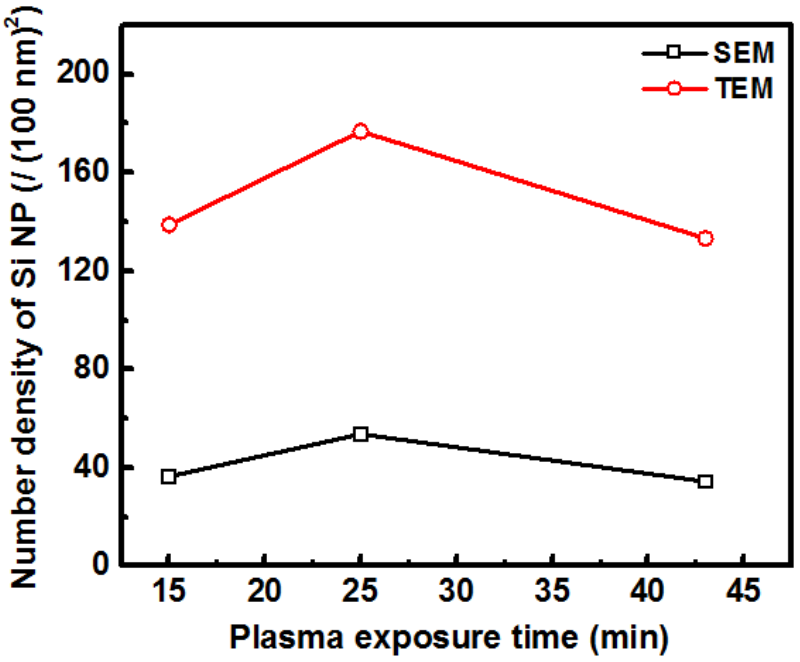


Fig) Number density of Si NP fabricated at RF bias of 9 W depending on plasma exposure time

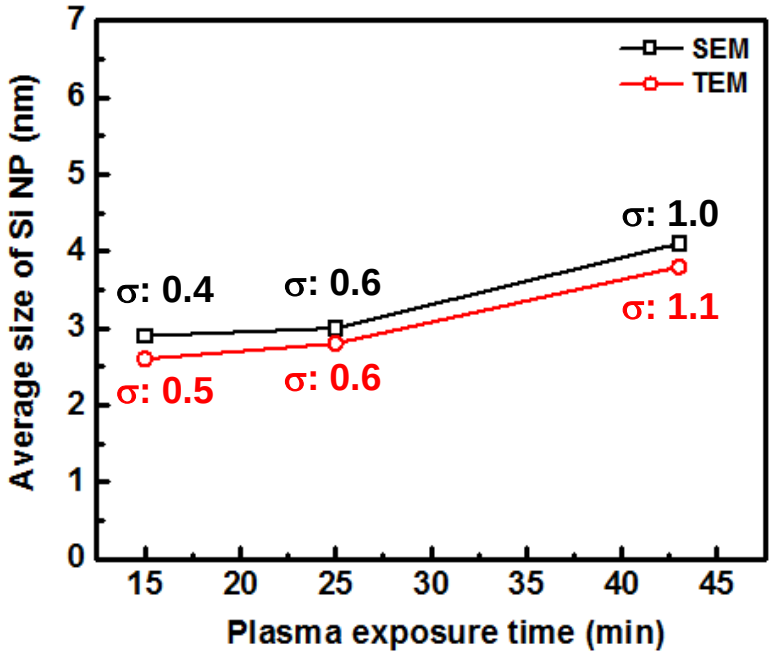
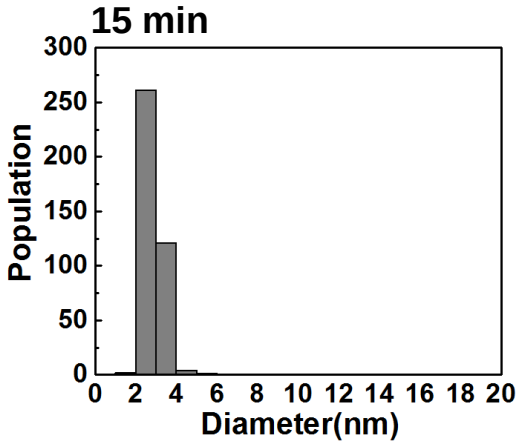


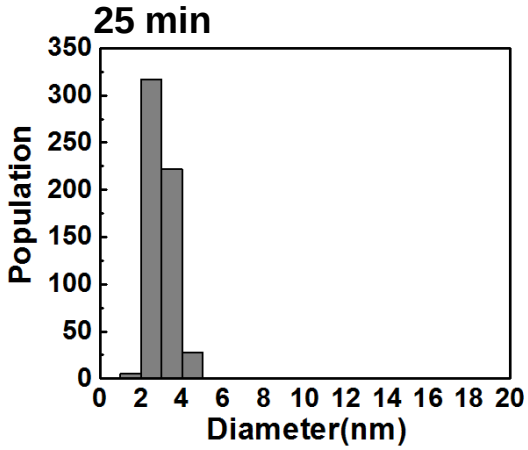
Fig) Average size of Si NP fabricated at RF bias of 9 W depending on plasma exposure time

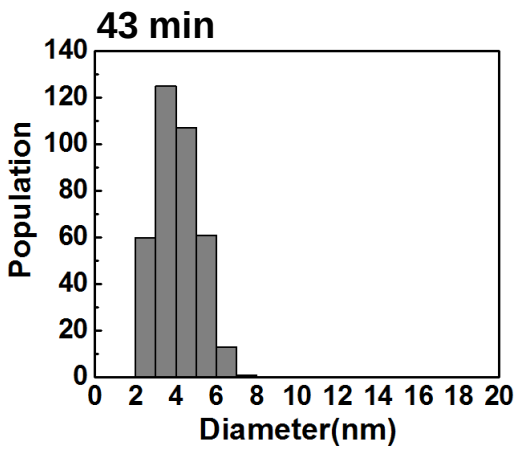
- Number density in TEM image is higher due to unexposed Si NPs under surface.
- Size of NP in TEM image is smaller due to unexposed Si NPs which are generated later.

Size distribution of Si NP in SEM and TEM images

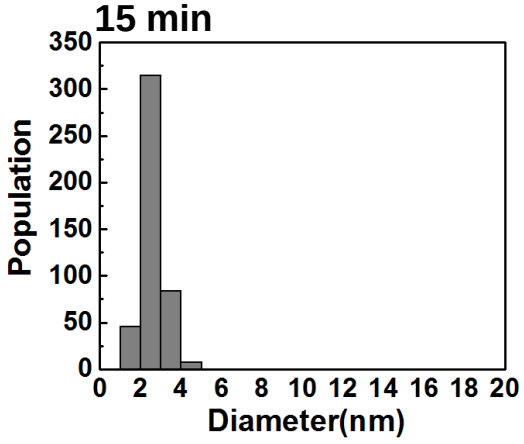
SEM

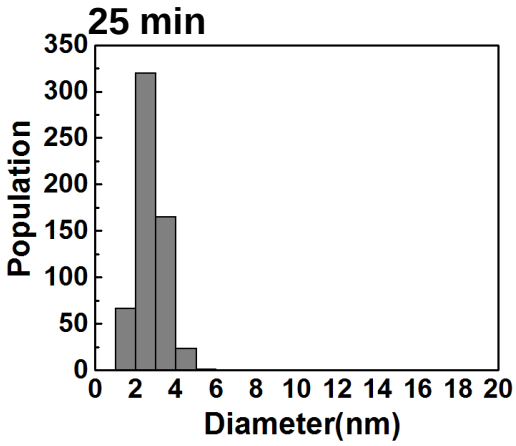


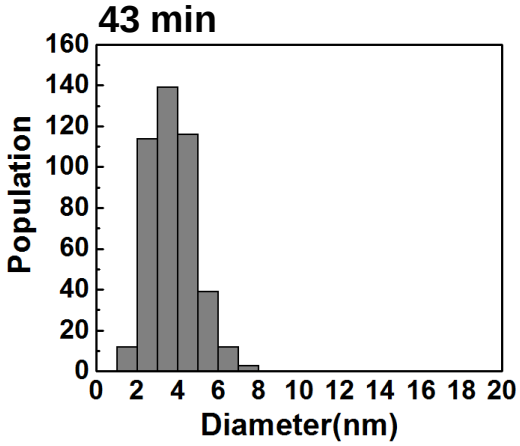




TEM

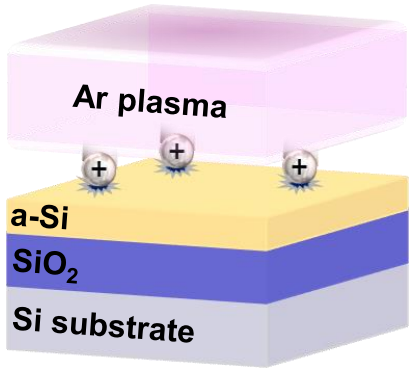






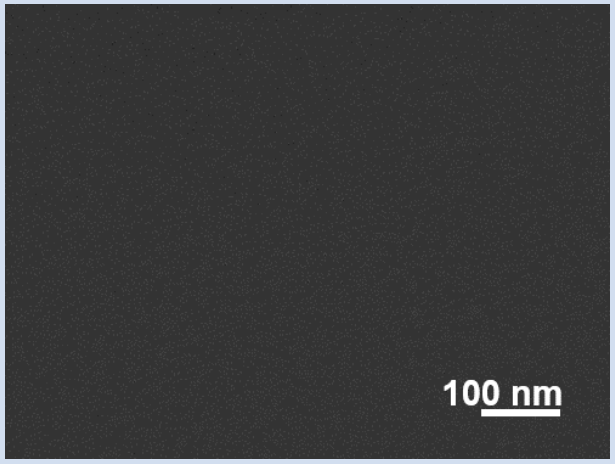
- Size of NP in TEM image is smaller due to unexposed Si NPs which are generated later.

Nucleation effect for generation of Si NP

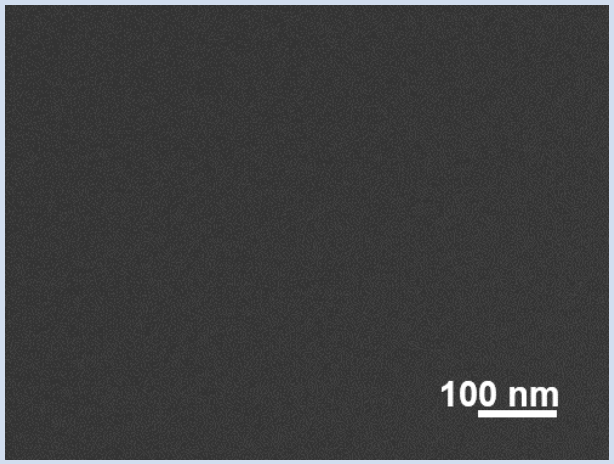


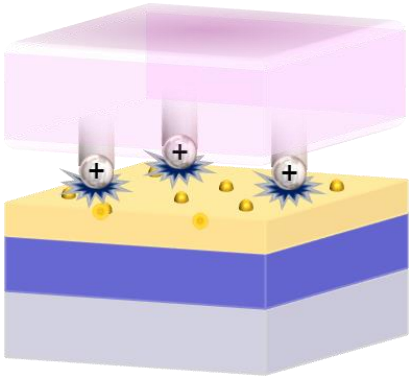
ICP without bias

W/O bias 10 min



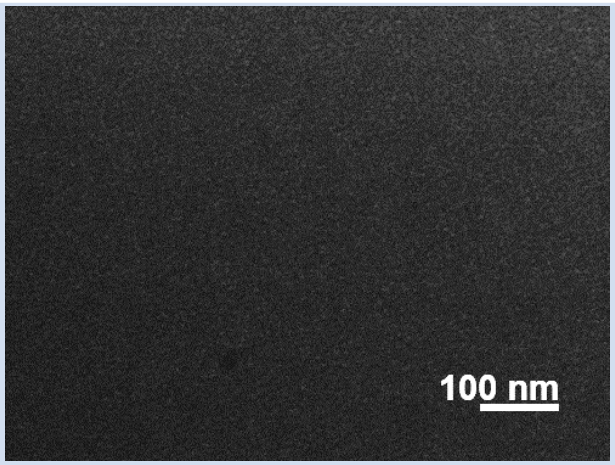
W/O bias 2 hr 10 min



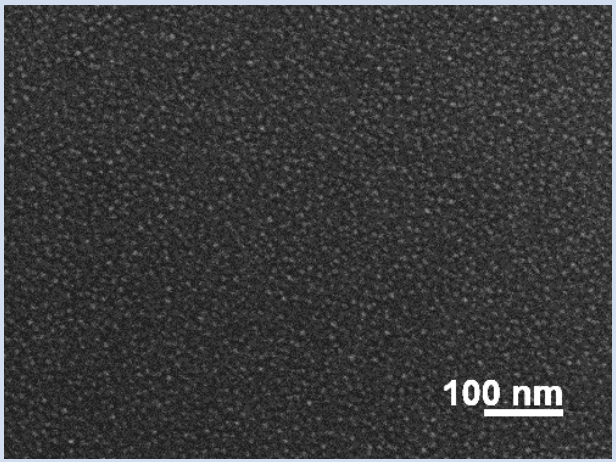


ICP with bias (9 W)

9 W 10 min



9 W 10 min + W/O bias 2 hr



➢ Nucleation of Si nanoseed by ion energy is important for generation of Si NP.

Ion kinetic energy penetration

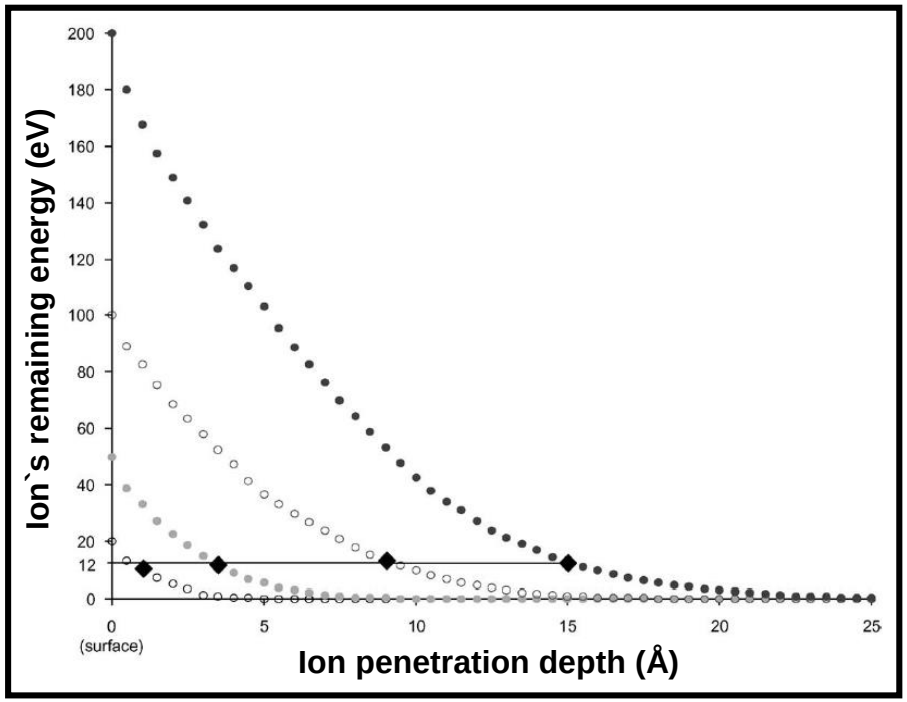


Fig) Ion remaining energy depending on depth for Ar^+ ion impacting Si at normal incidence

D.B. Graves et al., Appl. Surf. Sci., 192, 72 (2002)

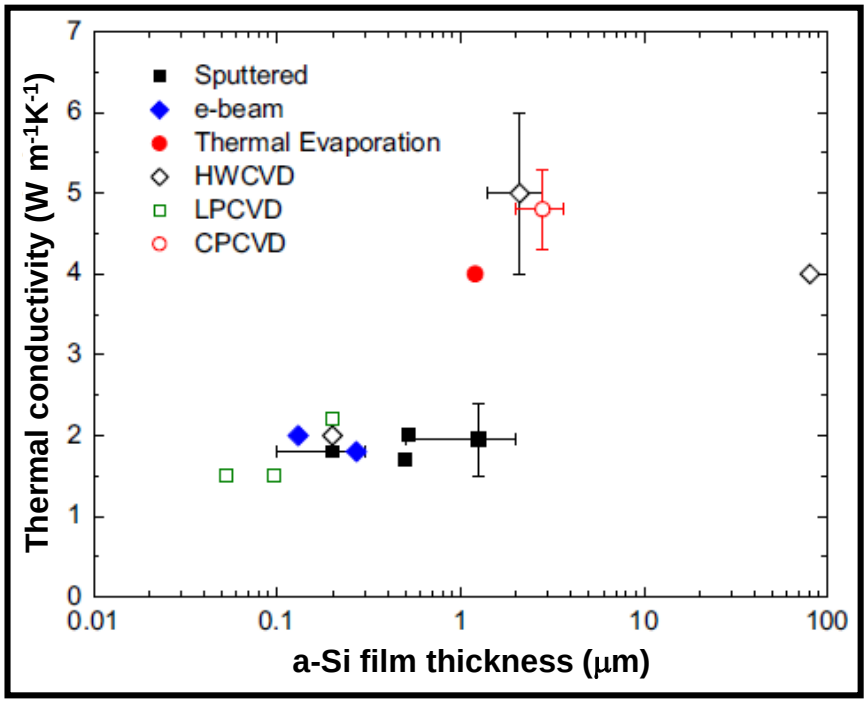


Fig) Literature data for thermal conductivity of a-Si as a function of film thickness

J.L.Braun et al., Phy. Rev. B 93, 140201(R) (2016)

- **Ar^+ ions below 100 eV can penetrate up to Si layer less than 1.5 nm thick.**
- **Thermal conductivity of a-Si is about 200 times smaller than that of metal due to local disorder and covalent bonding.**

Dot-structurization at surface of 30 nm-thick a-Si film

- **a-Si (30 nm)**

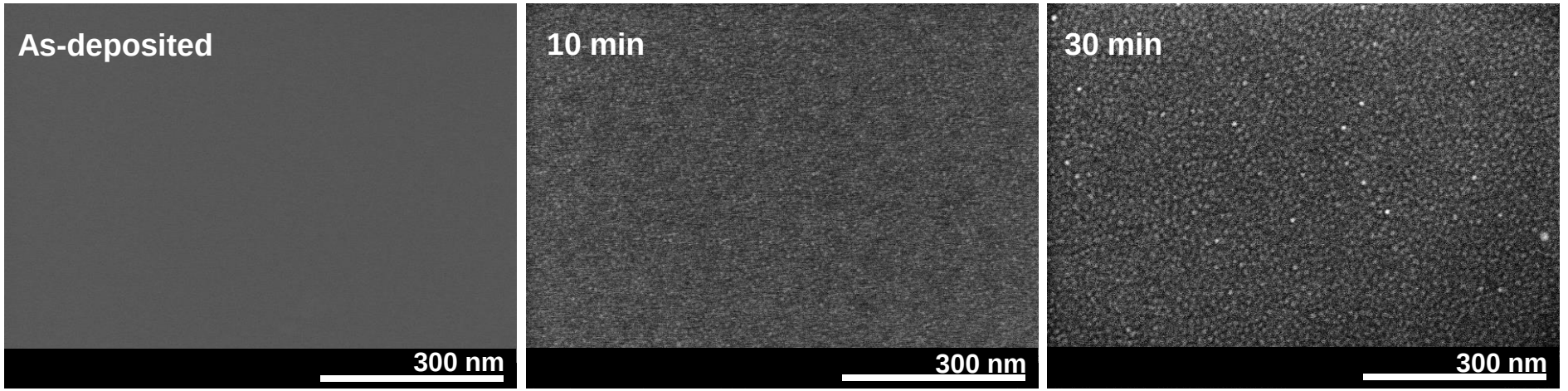
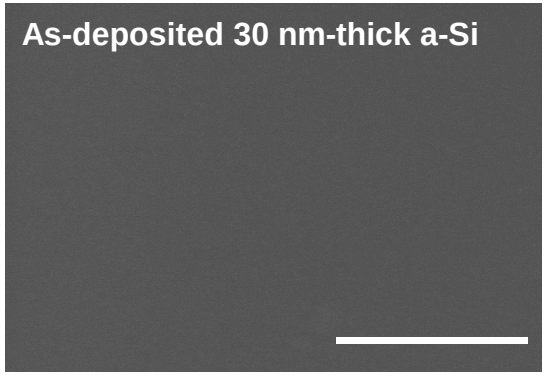
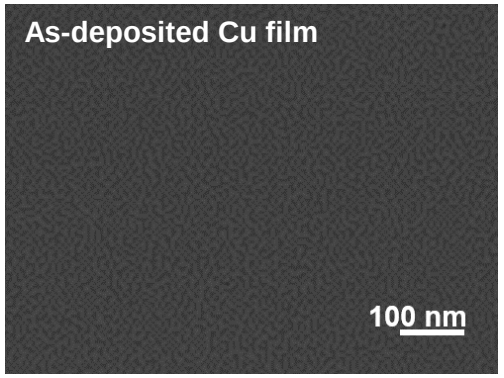


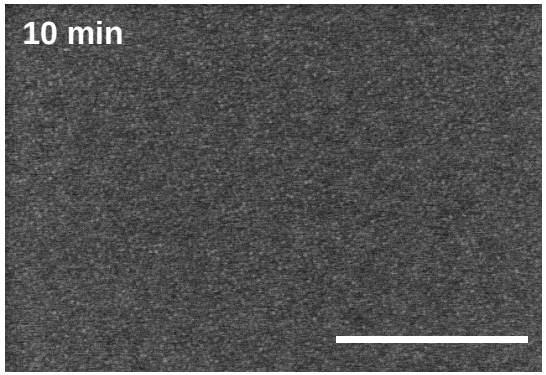
Fig) FE-SEM images of Si NPs on SiO_2/Si substrate fabricated at RF bias power of 9 W depending on plasma exposure time

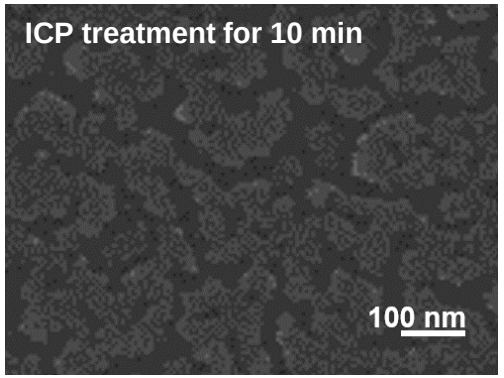
- **Nanoseeds were also created on surface of 30 nm-thick a-Si film.**
- **With increase in plasma treatment time, nanoseeds grew larger gradually.**

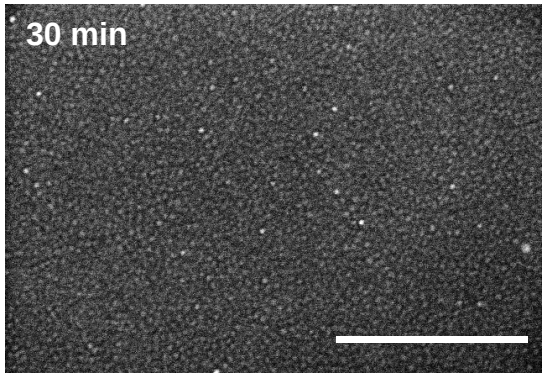
Comparison between a-Si and Cu

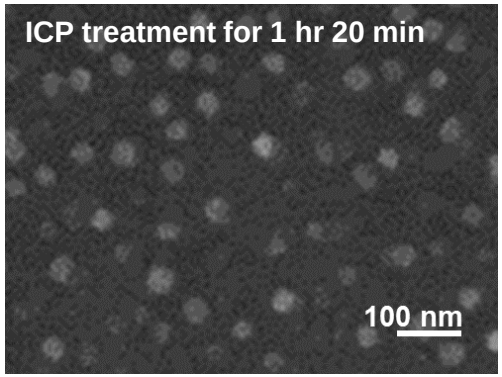












Nucleation of crystalline nanoseed (crystallization)

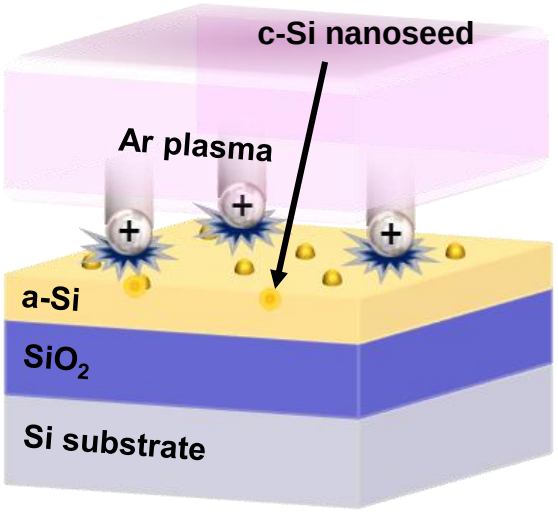
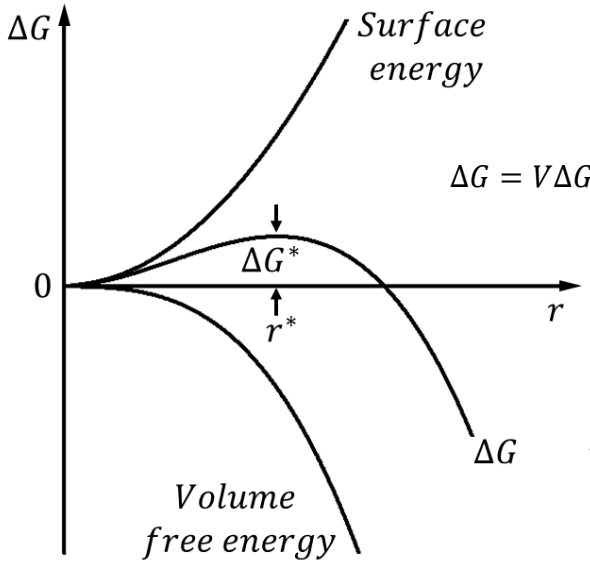


Fig) Schematic of Si nanoseed generation



$$\Delta G = V\Delta G_V + A_{ac}\gamma_{ac} - A_{aa}\gamma_{aa}$$

$$n^* = n_0 exp\left(-\frac{\Delta G^*}{kT}\right)$$

$$N = \omega n_0 \exp(-\frac{\Delta G_m}{kT}) exp\left(-\frac{\Delta G^*}{kT}\right)$$

Fig) Gibbs-free energy depending on radius of nuclei

D.A.Porter et al., Phase transformations in metals and alloys third edition (Boca Raton, FL: CRC Press) (2009)

- **Ar^+ ions bombard the a-Si film surface and transfer the ion energy.**
- **Energetic Si atoms form crystalline nanoseed (nuclei) by crystallization nucleation.**

Self-bias and plasma density with different RF bias power

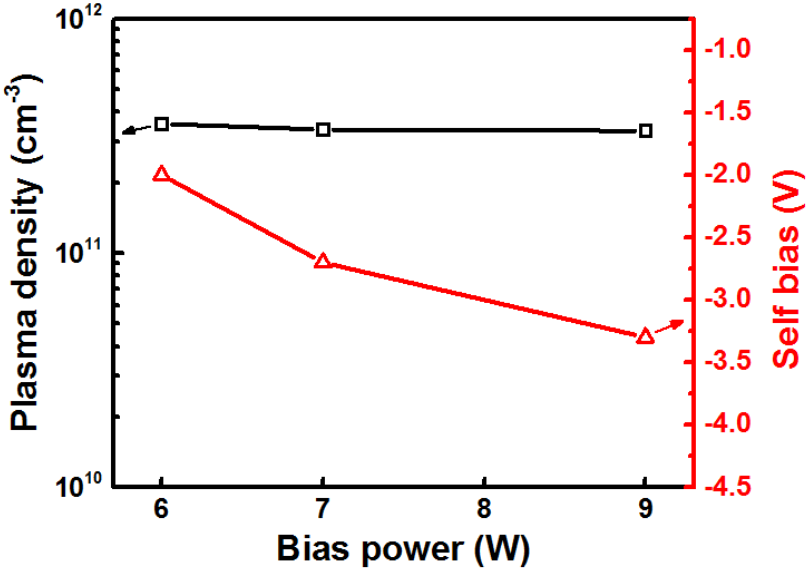


Fig) Measured plasma density and self-bias depending on RF bias power of substrate

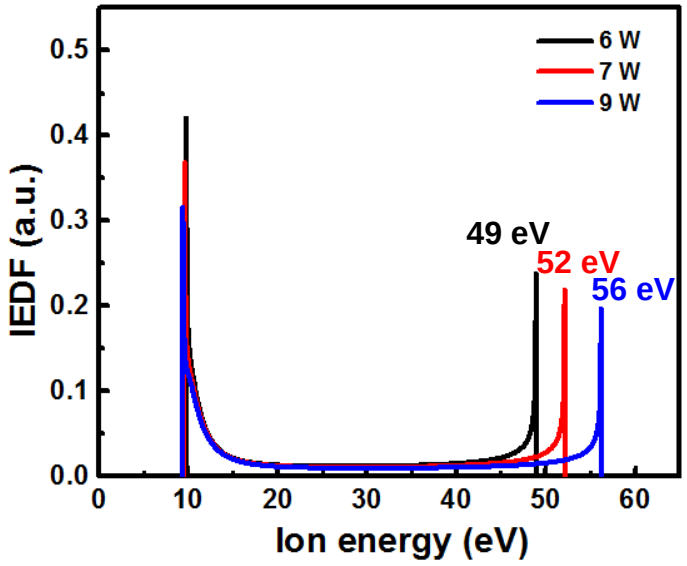
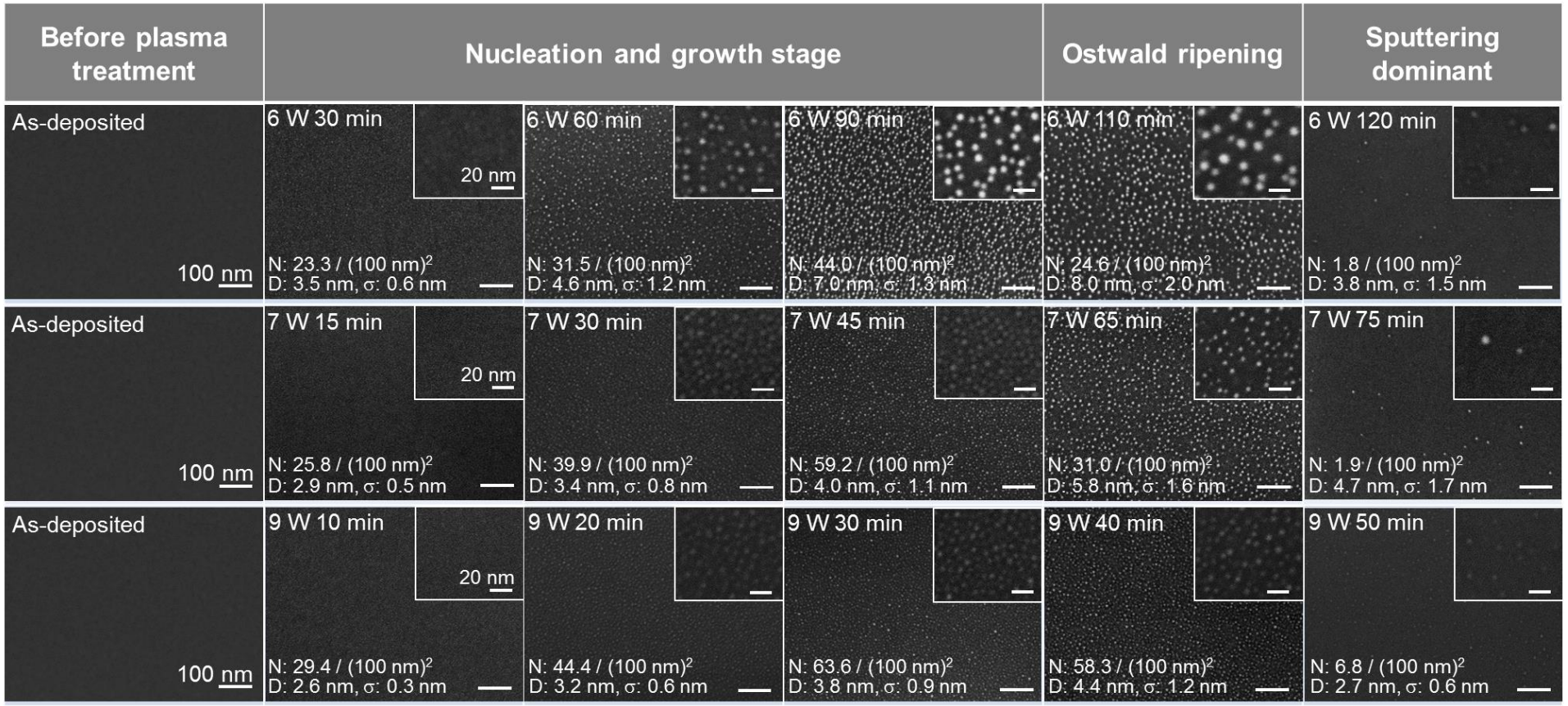


Fig) Calculated Ion energy distribution depending on RF bias power of substrate

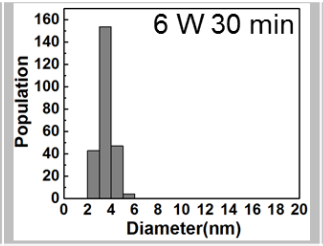
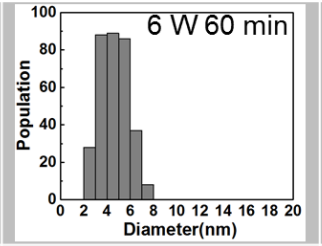
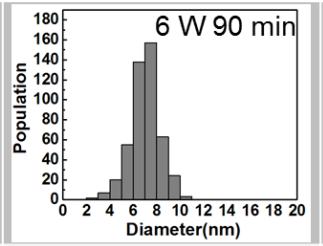
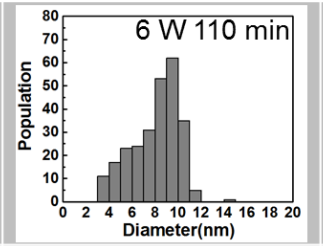
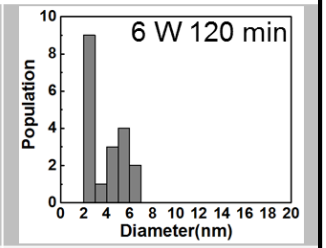
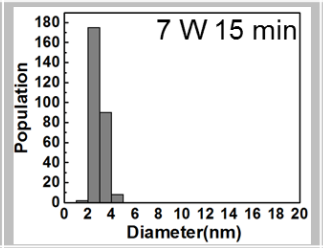
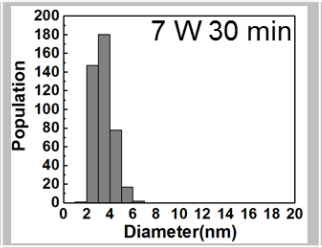
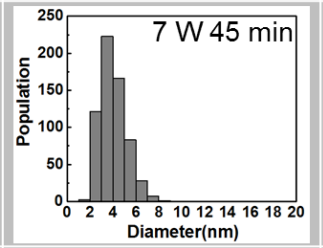
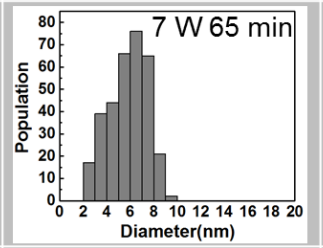
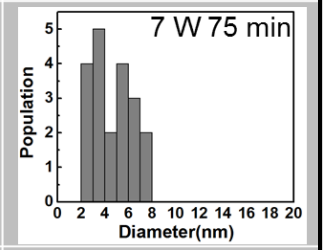
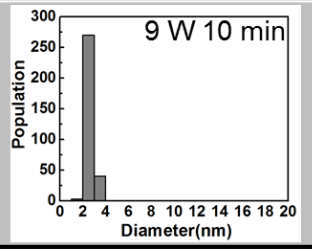
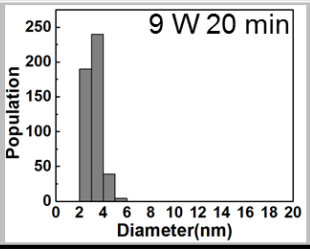
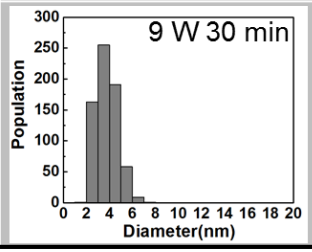
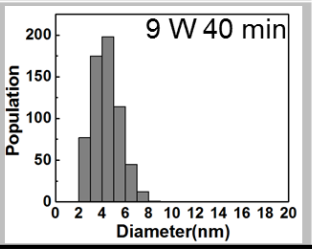
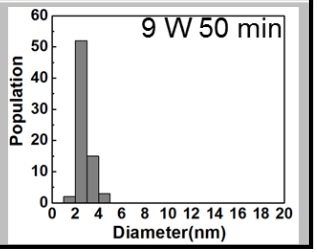
- The ion energy was increased with increasing RF bias in high energy range.
- High ion energy over threshold energy for sputtering (37.5 eV) can control the NP size.

Change of density and size of Si NP in different RF bias power condition



- **Nucleation and growth of Si NP occur due to ion bombardment energy.**
- **Size and density of Si NP are changed in different RF bias power condition.**

Size distribution of Si NP in different RF bias power condition

Before plasma treatment	Nucleation and growth stage			Ostwald ripening	Sputtering dominant
As-deposited					
As-deposited					
As-deposited					

- **The size of Si NPs decreased with increase in RF bias power.**
- **In Ostwald ripening stage, the uniformity of size decreased rapidly.**

Change of density and size of Si NP in different RF bias power condition

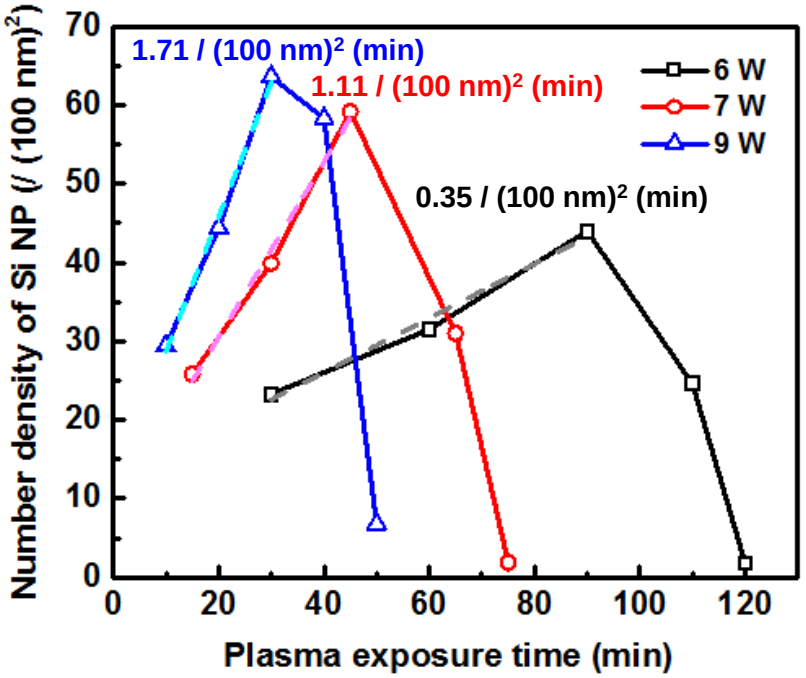


Fig) Number density of Si NP depending on plasma exposure time in different RF bias condition

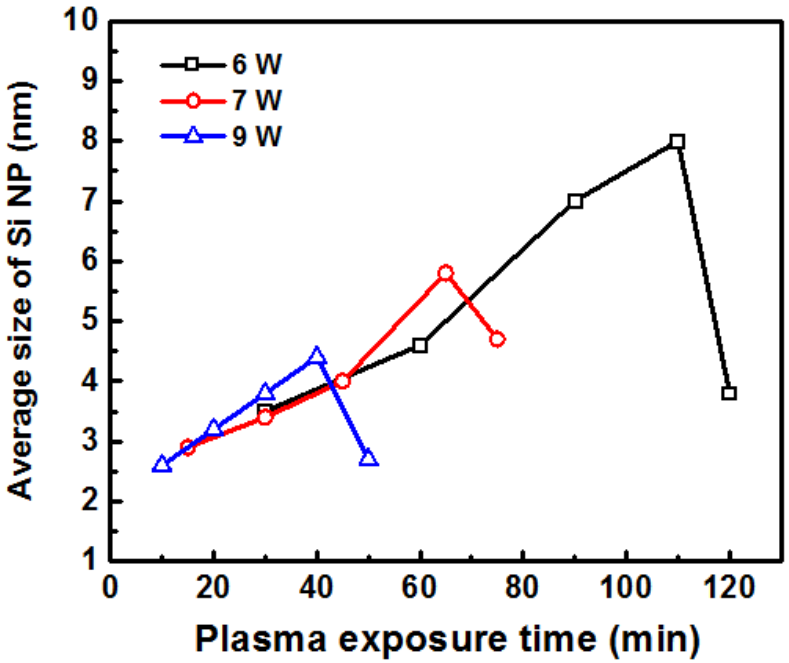


Fig) Average size of Si NP depending on plasma exposure time in different RF bias condition

- **Generation rate of Si NP increased with increase in RF bias power.**
- **Size of Si NP decreased with increase in RF bias power.**

Size control of Si NPs by change of RF bias of substrate electrode

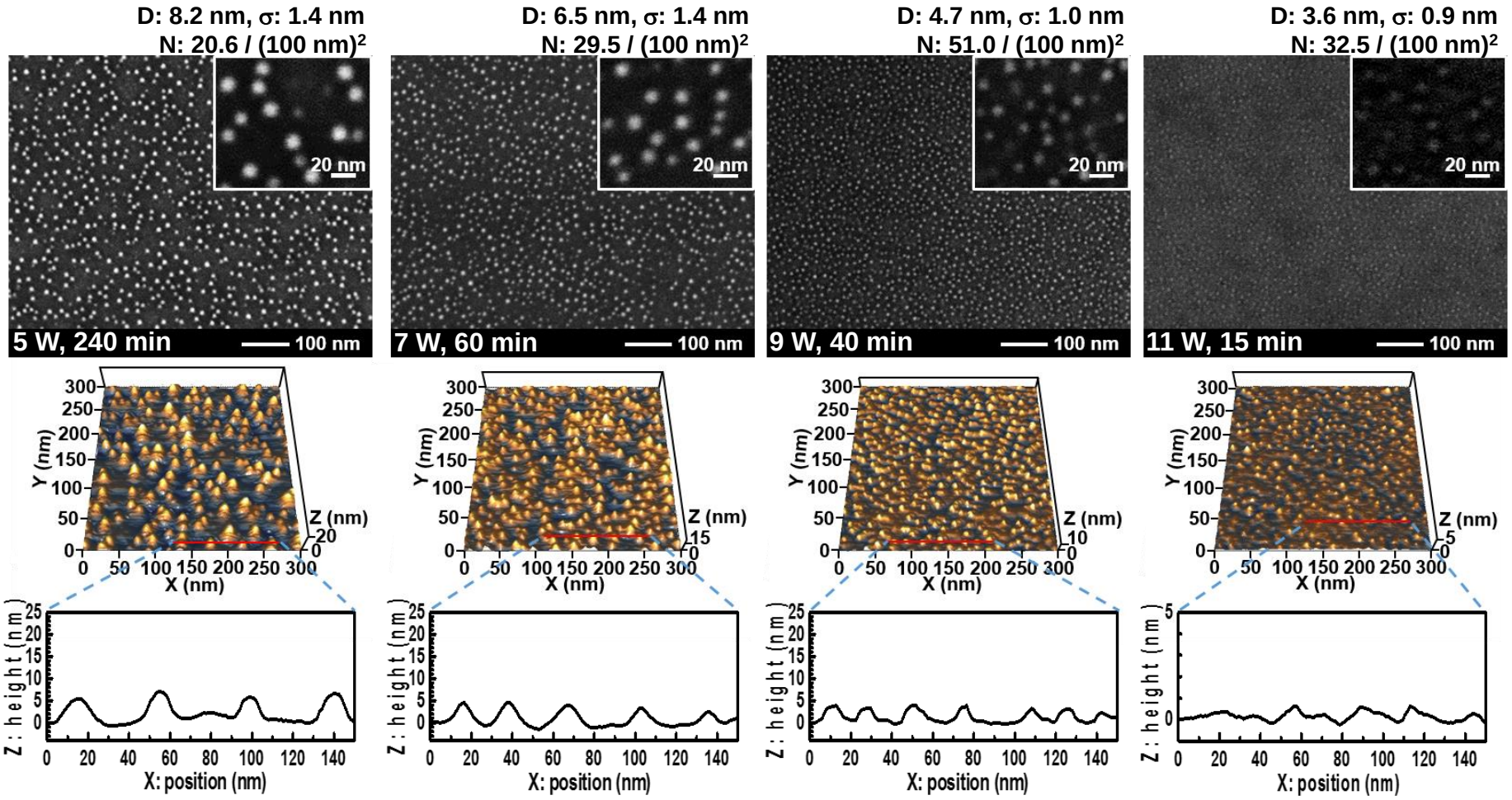
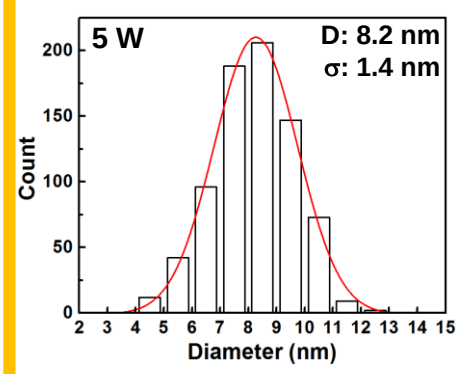


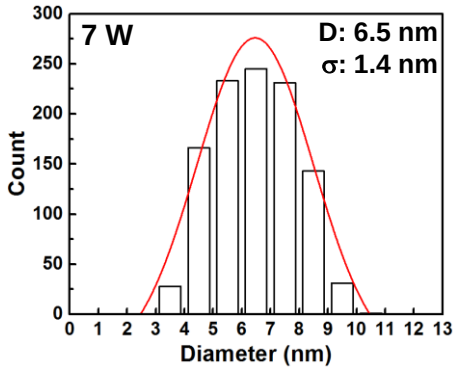
Fig) a-Si films after plasma treatment with different bias power and time

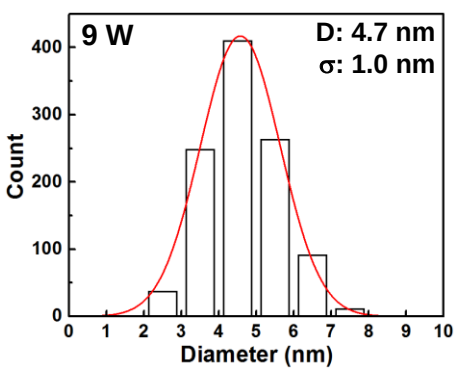
- **Size of Si NPs decreased with increase in bias power of substrate electrode.**
- **Fabrication time decreased efficiently.**

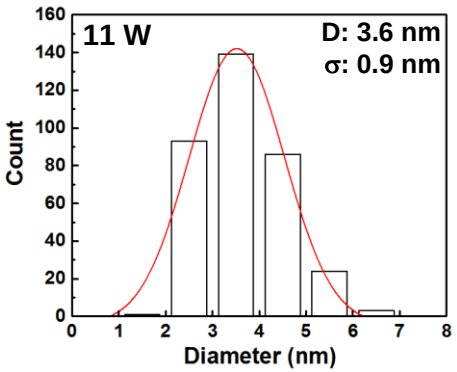
Size distribution of Si NPs and comparison with other results

➢ Plasma surface structurization

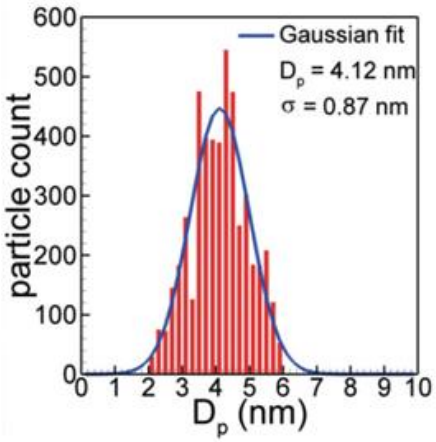






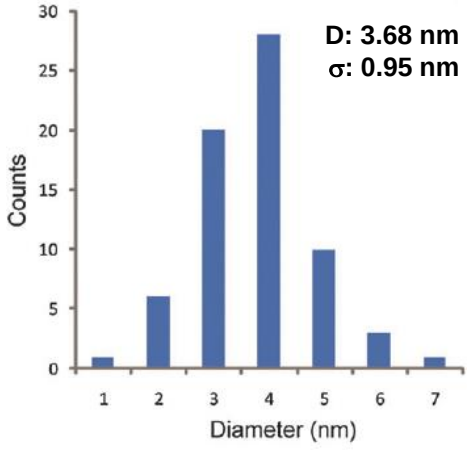


➢ Other results



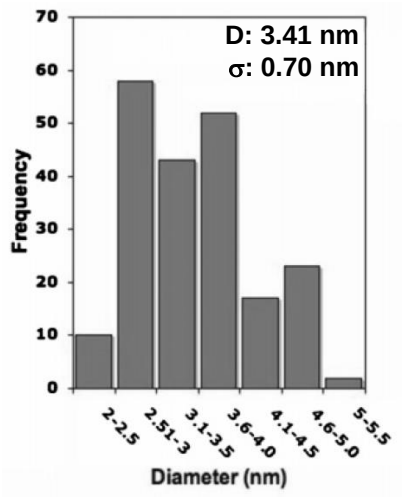
Gas discharge synthesis

L. Mangolini et al., Adv. Mater., 19, 2513 (2007)



Solution based precursor reduction method

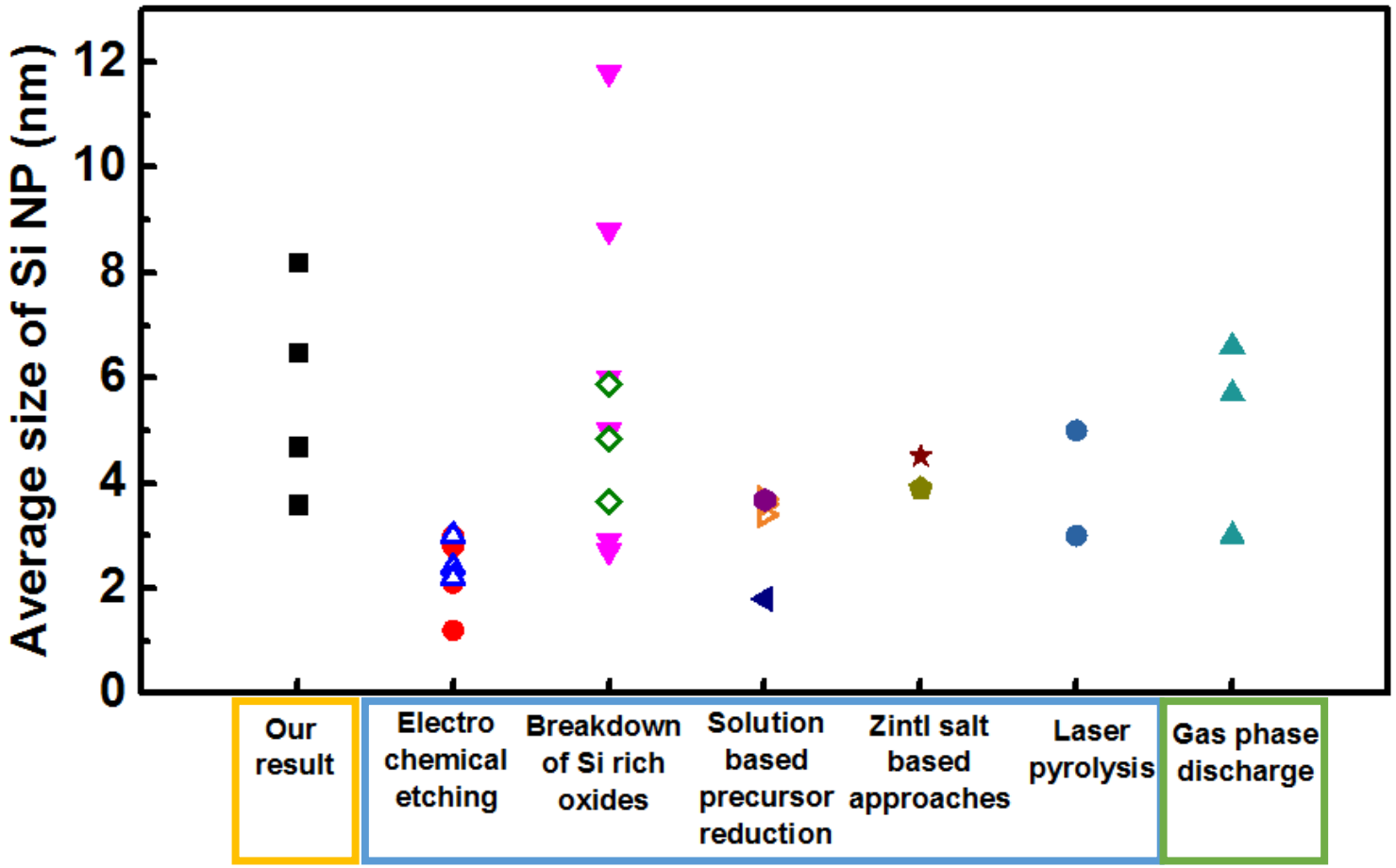
X.Cheng et al., Chem. Commun., 48, 11874 (2012)



Breakdown of Si rich oxides

Hessel et al., Chem. Mater., 18, 26 (2006)

Size of Si NPs for various fabrication methods



- Fabrication of Si NP was proceeded in non-toxic and low temperature environment.
- Size control was conducted in sub-10 nm range.

Summary

- **Crystalline Si nanoseeds are generated near surface region of a-Si.**
- **Crystalline Si nanoseeds were formed by nucleation and grew into crystalline Si NPs without a-Si thickness dependence.**
- **Size of Si NPs was controlled by changing RF bias of substrate electrode.**

Thank you!

LHC@kriss.re.kr